

MIT Open Access Articles

Measurement of the charge asymmetry in top quark pair production in pp collisions at $\sqrt{s}=7$ TeV using the ATLAS detector

The MIT Faculty has made this article openly available. **Please share** how this access benefits you. Your story matters.

Citation: The ATLAS Collaboration et al. "Measurement of the Charge Asymmetry in Top Quark Pair Production in Pp Collisions at $\sqrt{s}=7$ TeV Using the ATLAS Detector." The European Physical Journal C 72.6 (2012): n. pag. © 2012 CERN for the benefit of the ATLAS collaboration

As Published: <http://dx.doi.org/10.1140/epjc/s10052-012-2039-5>

Publisher: Springer-Verlag

Persistent URL: <http://hdl.handle.net/1721.1/106181>

Version: Final published version: final published article, as it appeared in a journal, conference proceedings, or other formally published context

Terms of use: Creative Commons Attribution 4.0 International License



Measurement of the charge asymmetry in top quark pair production in pp collisions at $\sqrt{s} = 7$ TeV using the ATLAS detector

The ATLAS Collaboration*

CERN, 1211 Geneva 23, Switzerland

Received: 19 March 2012 / Revised: 17 May 2012 / Published online: 15 June 2012

© CERN for the benefit of the ATLAS collaboration 2012. This article is published with open access at Springerlink.com

Abstract A measurement of the top-antitop production charge asymmetry A_C is presented using data corresponding to an integrated luminosity of 1.04 fb^{-1} of pp collisions at $\sqrt{s} = 7$ TeV collected by the ATLAS detector at the LHC. Events are selected with a single lepton (electron or muon), missing transverse momentum and at least four jets of which at least one jet is identified as coming from a b -quark. A kinematic fit is used to reconstruct the $t\bar{t}$ event topology. After background subtraction, a Bayesian unfolding procedure is performed to correct for acceptance and detector effects. The measured value of A_C is $A_C = -0.019 \pm 0.028$ (stat.) ± 0.024 (syst.), consistent with the prediction from the MC@NLO Monte Carlo generator of $A_C = 0.006 \pm 0.002$. Measurements of A_C in two ranges of invariant mass of the top-antitop pair are also shown.

1 Introduction

The top quark is the heaviest elementary particle so far observed. With a mass close to the electroweak scale it may play a special role in physics beyond the Standard Model (SM). Its pair production at hadron colliders allows a test of quantum chromodynamics (QCD) at high energies.

This paper describes the measurement of the charge asymmetry A_C , defined as [1, 2]:

$$A_C = \frac{N(\Delta|y| > 0) - N(\Delta|y| < 0)}{N(\Delta|y| > 0) + N(\Delta|y| < 0)}, \quad (1)$$

where $\Delta|y| \equiv |y_t| - |y_{\bar{t}}|$ is the difference between the absolute values of the top and antitop rapidities ($|y_t|$ and $|y_{\bar{t}}|$) and N is the number of events with $\Delta|y|$ positive or negative.

Although $t\bar{t}$ production at hadron colliders is predicted to be symmetric under the exchange of t and \bar{t} at leading

order, at next-to-leading order (NLO) the process $q\bar{q} \rightarrow t\bar{t}g$ exhibits an asymmetry in the differential distributions of the top and antitop, due to interference between initial and final state gluon emission. The $q\bar{q} \rightarrow t\bar{t}$ process also possesses an asymmetry due to the interference between the Born and box diagrams. Similarly, the $qg \rightarrow t\bar{t}q$ process is asymmetric due to interference between amplitudes which have a relative sign difference under the exchange of t and \bar{t} . The production of $t\bar{t}$ pairs by gluon-gluon fusion, $gg \rightarrow t\bar{t}$, on the other hand, is symmetric.

In $p\bar{p}$ collisions at the Tevatron, where top pairs are predominantly produced by quark-antiquark annihilation, perturbative QCD predicts that the top quark will be preferentially emitted in the direction of the incoming quark and the antitop in the direction of the incoming antiquark [3]. Consequently, the charge asymmetry is measured as a forward-backward asymmetry, A_{FB} . Recent measurements of A_{FB} by the CDF and D0 Collaborations [4–7] show a 2–3 σ excess over the SM expectations enhancing interest in scrutinising the $t\bar{t}$ asymmetry. For $t\bar{t}$ invariant mass, $m_{t\bar{t}}$, greater than 450 GeV, the CDF experiment measures an asymmetry in the $t\bar{t}$ rest frame which is 3.4 σ above the SM prediction [6]. Several new physics models have been proposed to explain the excess observed at CDF and D0 [1, 8–17]. Different models predict different asymmetries as a function of $m_{t\bar{t}}$ [18].

In pp collisions at the LHC, the dominant mechanism for $t\bar{t}$ production is expected to be the gluon-gluon fusion process, while $t\bar{t}$ production via $q\bar{q}$ or qg is small. Since the initial state is symmetric, the forward-backward asymmetry is no longer a useful observable. However, due to the asymmetry in the production via $q\bar{q}$ and qg , QCD predicts at the LHC a small excess of centrally produced antitop quarks while top quarks are produced, on average, at higher absolute rapidities. This can be understood by the fact that for $t\bar{t}$ production via $q\bar{q}$ annihilation the valence quark carries, on average, a larger momentum fraction than the anti-quark

* e-mail: atlas.publications@cern.ch

from the sea. With top quarks preferentially emitted in the direction of the initial quarks in the $t\bar{t}$ rest frame, the boost into the laboratory frame drives the top mainly in the forward or backward directions, while antitops are preferentially retained in the central region. If new physics is responsible for the Tevatron A_{FB} excess, the charge asymmetry measured at the LHC is a natural place to look for it.

In this paper, the measurement of the charge asymmetry A_C is performed using candidate $t\bar{t}$ events selected in the lepton + jets channel. In this channel, the SM decay of the $t\bar{t}$ pair to $W^+bW^-\bar{b}$ results in a single electron or muon from one of the W boson decays and four jets, two from the second W boson decay and two from the b - and \bar{b} -quarks. To allow comparisons with theory calculations, the measured $\Delta|y|$ distribution is unfolded to account for acceptance and detector effects. An inclusive measurement, and measurements of A_C in two ranges of $t\bar{t}$ invariant mass, are presented. An inclusive measurement of this asymmetry with an equivalent observable has been recently reported by the CMS collaboration [19].

2 The ATLAS detector

The ATLAS detector [20] at the LHC covers nearly the entire solid angle¹ around the collision point. It consists of an inner tracking detector surrounded by a thin superconducting solenoid, electromagnetic and hadronic calorimeters, and an external muon spectrometer incorporating three large superconducting toroid magnet assemblies.

The inner-detector system is immersed in a 2 T axial magnetic field and provides charged particle tracking in the range $|\eta| < 2.5$. The high-granularity silicon pixel detector covers the vertex region and provides typically three measurements per track, followed by the silicon microstrip tracker (SCT) which provides four measurements from eight strip layers. These silicon detectors are complemented by the transition radiation tracker (TRT), which enables extended track reconstruction up to $|\eta| = 2.0$. In giving typically more than 30 straw-tube measurements per track, the TRT improves the inner detector momentum resolution, and also provides electron identification information.

The calorimeter system covers the pseudorapidity range $|\eta| < 4.9$. Within the region $|\eta| < 3.2$, electromagnetic calorimetry is provided by barrel and endcap lead-liquid

argon (LAr) electromagnetic calorimeters, with an additional thin LAr presampler covering $|\eta| < 1.8$ to correct for energy loss in material upstream of the calorimeters. Hadronic calorimetry is provided by the steel/scintillating-tile calorimeter, segmented into three barrel structures within $|\eta| < 1.7$, and two copper/LAr hadronic endcap calorimeters. The solid angle coverage is completed with forward copper/LAr and tungsten/LAr calorimeter modules optimised for electromagnetic and hadronic measurements respectively.

The muon spectrometer comprises separate trigger and high-precision tracking chambers measuring the deflection of muons in a magnetic field with a bending integral from 2 to 8 Tm in the central region, generated by three superconducting air-core toroids. The precision chamber system covers the region $|\eta| < 2.7$ with three layers of monitored drift tubes, complemented by cathode strip chambers in the forward region, where the background is highest. The muon trigger system covers the range $|\eta| < 2.4$ with resistive plate chambers in the barrel, and thin gap chambers in the endcap regions.

A three-level trigger system is used to select interesting events. The level-1 trigger is implemented in hardware and uses a subset of detector information to reduce the event rate to a design value of at most 75 kHz. This is followed by two software-based trigger levels, level-2 and the event filter, which together reduce the event rate to about 300 Hz.

3 Data and Monte Carlo samples

Data from LHC pp collisions collected by the ATLAS detector between March and June 2011 are used in the analysis, corresponding to an integrated luminosity of 1.04 fb^{-1} .

Simulated top pair events are generated using the MC@NLO [21] Monte Carlo (MC) generator with the NLO parton density function (PDF) set CTEQ6.6 [22]. Parton showering and the underlying event are modelled using HERWIG [23] and JIMMY [24], respectively. This $t\bar{t}$ sample is normalised to a cross section of 165 pb, obtained with the latest theoretical computation, which approximates the next-to-next-to leading order prediction [25]. Single top events are also generated using MC@NLO while the production of W/Z bosons in association with jets is simulated using the ALPGEN generator [26] interfaced to HERWIG and JIMMY with CTEQ6.1 [27]. Diboson events (WW , WZ , ZZ) are generated using HERWIG with MRST2007lomod [28].

All Monte Carlo simulation samples are generated with multiple pp interactions per bunch crossing (pile-up). These simulated events are re-weighted so that the distribution of the number of interactions per crossing in simulation matches that in the data. The samples are then processed through the GEANT4 [29] simulation [30] of the ATLAS detector and the standard reconstruction software.

¹ATLAS uses a right-handed coordinate system with its origin at the nominal interaction point (IP) in the centre of the detector and the z -axis along the beam pipe. The x -axis points from the IP to the centre of the LHC ring, and the y axis points upward. Cylindrical coordinates (r, ϕ) are used in the transverse plane, ϕ being the azimuthal angle around the beam pipe. The pseudorapidity is defined in terms of the polar angle θ as $\eta = -\ln \tan(\theta/2)$. Transverse momentum and energy are defined as $p_T = p \sin \theta$ and $E_T = E \sin \theta$, respectively.

4 Event selection

4.1 Physics object selection

Reconstructing top quark pair events in the detector requires electrons, muons, jets and missing momentum to be simultaneously measured. Electron candidates are defined as energy deposits in the electromagnetic calorimeter associated with a well-measured track. Identification criteria based on shower shape variables, track quality, and information from the transition radiation tracker are applied to electron candidates [31]. All candidates are required to have $p_T > 25$ GeV and $|\eta_{\text{cluster}}| < 2.47$, where η_{cluster} is the pseudorapidity of the electromagnetic calorimeter cluster associated with the electron. Candidates in the calorimeter transition region $1.37 < |\eta_{\text{cluster}}| < 1.52$ are excluded.

Muon candidates are reconstructed from track segments in different layers of the muon chambers. These segments are combined starting from the outermost layer, with a procedure that takes material effects into account, and matched with tracks found in the inner detector. The candidates are then refitted using the complete track information from both detector systems, and are required to satisfy $p_T > 20$ GeV and $|\eta| < 2.5$.

Jets are reconstructed with the anti- k_r algorithm, with a distance parameter of 0.4 [32], starting from clusters of energy in adjacent calorimeter cells at the electromagnetic (EM) scale. The jet energy is corrected to the hadronic scale using p_T - and η -dependent correction factors obtained from simulation and validated with data [33]. Jet quality criteria are applied to identify jets not associated to in-time real energy deposits in the calorimeters caused by various sources (calorimeter noise, non-collision beam-related background, cosmic-ray induced showers).

The missing transverse momentum (E_T^{miss}) is reconstructed from clusters of energy calibrated at the EM scale and corrected according to the energy scale of the associated physics object [34]. Contributions from muons are included using their momentum measured from the tracking and muon spectrometer systems. The remaining clusters not associated with the high p_T objects are also included in the missing transverse momentum.

Muons within $\Delta R = 0.4$ of a jet axis² and with $p_T > 20$ GeV are removed in order to reduce the contamination caused by muons from hadron decays. Subsequently, jets within $\Delta R = 0.2$ of an electron candidate are removed to avoid double counting electrons as jets.

Isolation criteria are applied to both electron and muon candidates to reduce the backgrounds from hadrons mimicking lepton signatures and backgrounds from heavy flavour

decays inside jets. For electrons, the total energy in a cone of $\Delta R = 0.2$ around the electron candidate must not exceed 3.5 GeV, after correcting for energy deposits from pile-up and for the energy associated with the electron. For muons, the sum of track transverse momenta for all tracks with $p_T > 1$ GeV and the total energy deposited in a cone of $\Delta R = 0.3$ around the muon are both required to be less than 4 GeV ignoring the contribution of the muon p_T .

Reconstructing top quark pair events is facilitated by the ability to tag jets from the hadronisation of b -quarks. For this purpose, two b -tagging algorithms are used and their results are combined to extract a tagging decision for each jet. One b -tagger exploits the topology of b - and c -hadron weak decays inside the jet. A Kalman filter [35] is used to find a common line on which the primary vertex and the b - and c -hadron decay vertices lie, as well as their position on this line, giving an approximate flight path for the b - and c -hadrons. The discrimination between b -, c - and light quark jets is based on a likelihood using the masses, momenta, flight-length significances, and track multiplicities of the reconstructed vertices as inputs. To further increase the flavour discrimination power, a second b -tagger is run which does not attempt to directly reconstruct decay vertices. Instead, this second tagger uses the transverse and the longitudinal impact parameter significances of each track within the jet to determine a likelihood that the jet originates from a b -quark. The results of both taggers are combined using a neural network to determine a single discriminant variable which is used to make tagging decisions. The combined tagger operating point chosen for the present analysis corresponds to a 70 % tagging efficiency for b -jets in simulated $t\bar{t}$ events while light flavour jets are suppressed by approximately a factor of 100.

4.2 Selection of $t\bar{t}$ candidates

The $t\bar{t}$ final state in the lepton + jets channel is characterised by an isolated lepton (electron or muon) with relatively high p_T , missing transverse momentum arising from the neutrino from the leptonic W decay, two b -quark jets and two light quark jets from the hadronic W decay. To select events with this topology, the appropriate single-electron or single-muon trigger is required to have fired (with thresholds at 20 and 18 GeV respectively). The events are also required to contain one and only one reconstructed lepton with $p_T > 25$ GeV for electrons and $p_T > 20$ GeV for muons. To reject multijet background in the muon channel, $E_T^{\text{miss}} > 20$ GeV and $E_T^{\text{miss}} + m_T(W) > 60$ GeV are required.³ In the electron channel more stringent cuts on E_T^{miss} and $m_T(W)$

² $\Delta R = \sqrt{\Delta\phi^2 + \Delta\eta^2}$, where $\Delta\phi$ and $\Delta\eta$ are the separation in azimuthal angle and pseudorapidity, respectively.

³Here $m_T(W)$ is the W -boson transverse mass, defined as $\sqrt{2p_T^\ell p_T^\nu (1 - \cos(\phi^\ell - \phi^\nu))}$ where the measured E_T^{miss} vector provides the neutrino information.

are required because of the higher level of multijet background, i.e. $E_T^{\text{miss}} > 35$ GeV and $m_T(W) > 25$ GeV. Events are required to have at least four jets with $p_T > 25$ GeV and $|\eta| < 2.5$. These requirements define the ‘pretag’ selection. The ‘tagged’ selection requires, in addition, at least one of the jets with $p_T > 25$ GeV and $|\eta| < 2.5$ to be b -tagged.

5 Background determination

5.1 Multijet background

The method used for evaluating the multijet background with fake leptons⁴ in both the electron and muon channels is the so-called ‘Matrix Method’. This relies on defining loose and tight lepton samples [36] and measuring the fractions of real (ϵ_{real}) and fake (ϵ_{fake}) loose leptons that are selected as tight leptons. The fraction ϵ_{real} is measured using data control samples of Z boson decays to two leptons, while ϵ_{fake} is measured from data control regions defined separately for the electron and muon channels, where the contribution of fake leptons is dominant.

For the muon channel, the loose data sample is defined by removing the isolation requirements in the default muon selection. The fake lepton efficiencies are determined using a low m_T control region $m_T < 20$ GeV with an additional cut $E_T^{\text{miss}} + m_T < 60$ GeV. The efficiencies for signal and fake leptons are parameterised as a function of muon $|\eta|$ and p_T in order to account for the variation of the muon detector acceptance and the profile of hadronic activity in the detector that affects the muon isolation.

For the multijet background estimate in the electron channel, the loose data sample is defined by considering events with electrons passing looser identification criteria. The electron isolation requirement is also modified: the total energy in a cone of $\Delta R = 0.2$ around the electron is required to be smaller than 6 GeV (instead of 3.5 GeV), after correcting for energy deposits from pile-up interactions and for the energy associated with the electron. The fake lepton efficiencies are determined using a low E_T^{miss} control region ($5 \text{ GeV} < E_T^{\text{miss}} < 20 \text{ GeV}$).

In both channels contributions from W + jets and Z + jets backgrounds in the control region, estimated using Monte Carlo simulation, are subtracted.

5.2 W + jets background estimation

At the LHC the rate of W^+ + jets is larger than that of W^- + jets because there are more valence u quarks than

d quarks in the proton. Theoretically, the ratio of W^+ + jets and W^- + jets cross sections is predicted much more precisely than the total W + jets cross section [37, 38]. This asymmetry is exploited here to measure the total W + jets background from the data.

Since, to a good approximation, processes other than W + jets give equal numbers of positively and negatively charged leptons, the formula

$$N_{W^+} + N_{W^-} = \left(\frac{r_{\text{MC}} + 1}{r_{\text{MC}} - 1} \right) (D^+ - D^-), \quad (2)$$

can be used to estimate the total number of W events in the selected sample. Here $D^+(D^-)$ are the total numbers of events in data passing the selection cuts described in Sect. 4.2 (apart from the b -tagging requirement) with positively (negatively) charged leptons, and $r_{\text{MC}} \equiv \frac{N(pp \rightarrow W^+)}{N(pp \rightarrow W^-)}$ is evaluated from Monte Carlo simulation, using the same event selection.

The ratio r_{MC} is found to be 1.56 ± 0.06 in the electron channel and 1.65 ± 0.08 in the muon channel. The dominant uncertainties on r_{MC} originate from those of the parton distribution functions, the jet energy scale, and the heavy flavour fractions in W + jets events (fractions of W + jets events containing $b\bar{b}$ pairs, $c\bar{c}$ pairs and c quarks).

Since the theoretical prediction for heavy flavour fractions in W + jets suffers from large uncertainties, a data-driven approach was developed to constrain these fractions with some inputs from MC simulation. In this approach samples with a lower jet multiplicity, obtained from the selection described in Sect. 4.2, but requiring precisely one or two jets instead of four or more jets, are analysed. The numbers $W_{i,\text{pretag}}^{\text{Data}}$, $W_{i,\text{tagged}}^{\text{Data}}$ of W + i jet events in these samples (where $i = 1, 2$), before and after applying the b -tagging requirement, are computed by subtracting the small contributions of other Standard Model processes—electroweak (WW , WZ , ZZ and Z + jets) and top ($t\bar{t}$ and single top) using predictions from the simulation, and by subtracting the multijet background as described in Sect. 5.1.

A system of two equations, expressing the number of W + 1 jet events and W + 2 jets events before and after b -tagging, can be written with six independent flavour fractions as the unknowns, corresponding to fractions of $Wb\bar{b}$ + jets, $Wc\bar{c}$ + jets, and Wc + jets events in the one and two jet bins. The simulation prediction for the ratio of the heavy flavour fractions between the one and two jet bins is used to relate the heavy flavour fractions in the two bins, reducing the number of independent fractions to three. Finally, the ratio of the fractions of $Wc\bar{c}$ + jets and $Wb\bar{b}$ + jets events in the two-jet bin is taken to be fixed to the value obtained from simulated events in order to obtain two equations for two independent fractions. Based on this measurement, the heavy flavour fractions in simulated W + jets events are adjusted by a scale factor 1.63 ± 0.76

⁴The term ‘fake’ leptons here refers to hadrons mimicking lepton signatures and to leptons arising from heavy hadron decays, whereas ‘real’ leptons come from W and Z decays.

Table 1 Numbers of events observed in data and expected from $t\bar{t}$ signal events and various background processes for the pretag and tagged samples defined in Sect. 4.2. The experimentally determined uncertainties quoted for $W + \text{jets}$ and multijet backgrounds include systematic uncertainties on the normalisation. The quoted uncertain-

ties on the other backgrounds are those from theory, taken to be 8 % for $t\bar{t}$ and single top, 34 % for $Z + \text{jets}$ and 5 % for diboson backgrounds. The numbers correspond to an integrated luminosity of 1.04 fb^{-1} in both electron and muon channels

Channel	$\mu + \text{jets pretag}$	$\mu + \text{jets tagged}$	$e + \text{jets pretag}$	$e + \text{jets tagged}$
$t\bar{t}$	7200 ± 600	6300 ± 500	4800 ± 400	4260 ± 350
$W + \text{jets}$	8600 ± 1200	1390 ± 310	5400 ± 800	880 ± 200
Single top	460 ± 40	366 ± 32	320 ± 28	256 ± 22
$Z + \text{jets}$	940 ± 330	134 ± 47	760 ± 270	110 ± 40
Diboson	134 ± 7	22 ± 2	80 ± 5	13 ± 1
Multijets	1500 ± 800	500 ± 500	900 ± 500	250 ± 250
Total background	11700 ± 1400	2400 ± 600	7500 ± 900	1500 ± 320
Signal + background	18900 ± 1600	8800 ± 800	12000 ± 1000	5800 ± 500
Observed	19639	9124	12096	5829

for $Wb\bar{b} + \text{jets}$ and $Wc\bar{c} + \text{jets}$ events and 1.11 ± 0.35 for $Wc + \text{jets}$. When applied to the signal region, an additional 25 % uncertainty on these fractions is added, corresponding to the uncertainty of the Monte Carlo prediction for the ratio of heavy flavour fractions in different jet multiplicities. The heavy flavour scale factors are applied to simulated $W + \text{jets}$ events throughout this paper, and the effect of their uncertainties on the value of r_{MC} is evaluated.

Using (2), the total number of $W + \text{jets}$ events passing the event selection described in Sect. 4.2 without requiring a b -tagged jet, $W_{\geq 4, \text{pretag}}$, is evaluated to be 5400 ± 800 (stat. + syst.) in the electron channel and 8600 ± 1200 (stat. + syst.) in the muon channel.

The number of $W + \text{jets}$ events passing the selection with at least one b -tagged jet is subsequently evaluated as [36]

$$W_{\geq 4, \text{tagged}} = W_{\geq 4, \text{pretag}} \cdot f_{2, \text{tagged}} \cdot k_{2 \rightarrow \geq 4}. \quad (3)$$

Here $f_{2, \text{tagged}} \equiv W_{2, \text{tagged}}^{\text{Data}} / W_{2, \text{pretag}}^{\text{Data}}$ is the fraction of $W + 2$ jets events passing the requirement of having at least one b -tagged jet, and $k_{2 \rightarrow \geq 4} \equiv f_{\geq 4, \text{tagged}}^{\text{MC}} / f_{2, \text{tagged}}^{\text{MC}}$ is the ratio of the fractions of simulated $W + \text{jets}$ events passing the requirement of at least one b -tagged jet, for at least four and two jets, respectively. The value of $f_{2, \text{tagged}}$ is found to be 0.065 ± 0.005 in the electron and 0.069 ± 0.005 in the muon channel, where the uncertainties include statistical and systematic contributions. The ratio $k_{2 \rightarrow \geq 4}$ is found to be 2.52 ± 0.36 in the electron channel and 2.35 ± 0.34 in the muon channel. The uncertainties include both systematic contributions and contributions arising from the limited number of simulated events. The total number of $W + \text{jets}$ events passing the selection with a b -tagged jet, $W_{\geq 4, \text{tagged}}$, is evaluated to be 880 ± 200 (stat. + syst.) in the electron channel and 1390 ± 310 (stat. + syst.) in the muon channel.

5.3 Other backgrounds

The numbers of background events coming from single top production, $Z + \text{jets}$ and diboson events are evaluated using Monte Carlo simulation normalised to the relevant NNLO cross sections for single top and $Z + \text{jets}$ events and NLO for diboson events.

5.4 Event yield

The final numbers of expected and observed data events in both channels after the full event selection are listed in Table 1. The number of events in the electron channel is significantly lower than in the muon channel due to the higher lepton p_{T} requirement and the more stringent missing momentum requirement, which are necessary to reduce the contribution from the multijet background. The overall agreement between expectation and data is good.

6 Reconstruction of the $t\bar{t}$ final state

To measure the charge asymmetry in top pair events, the full $t\bar{t}$ system is reconstructed. For this purpose, a kinematic fit is used that assesses the compatibility of the observed event with the decays of a top-antitop pair based on a likelihood approach.

The likelihood takes as inputs the measured energies, pseudorapidities and azimuthal angles of four jets, the measured energy of the lepton, and the missing transverse momentum. If there are more than four jets in the event satisfying $p_{\text{T}} > 25 \text{ GeV}$ and $|\eta| < 2.5$, all subsets of four jets from the five jets in the event with highest p_{T} are considered.

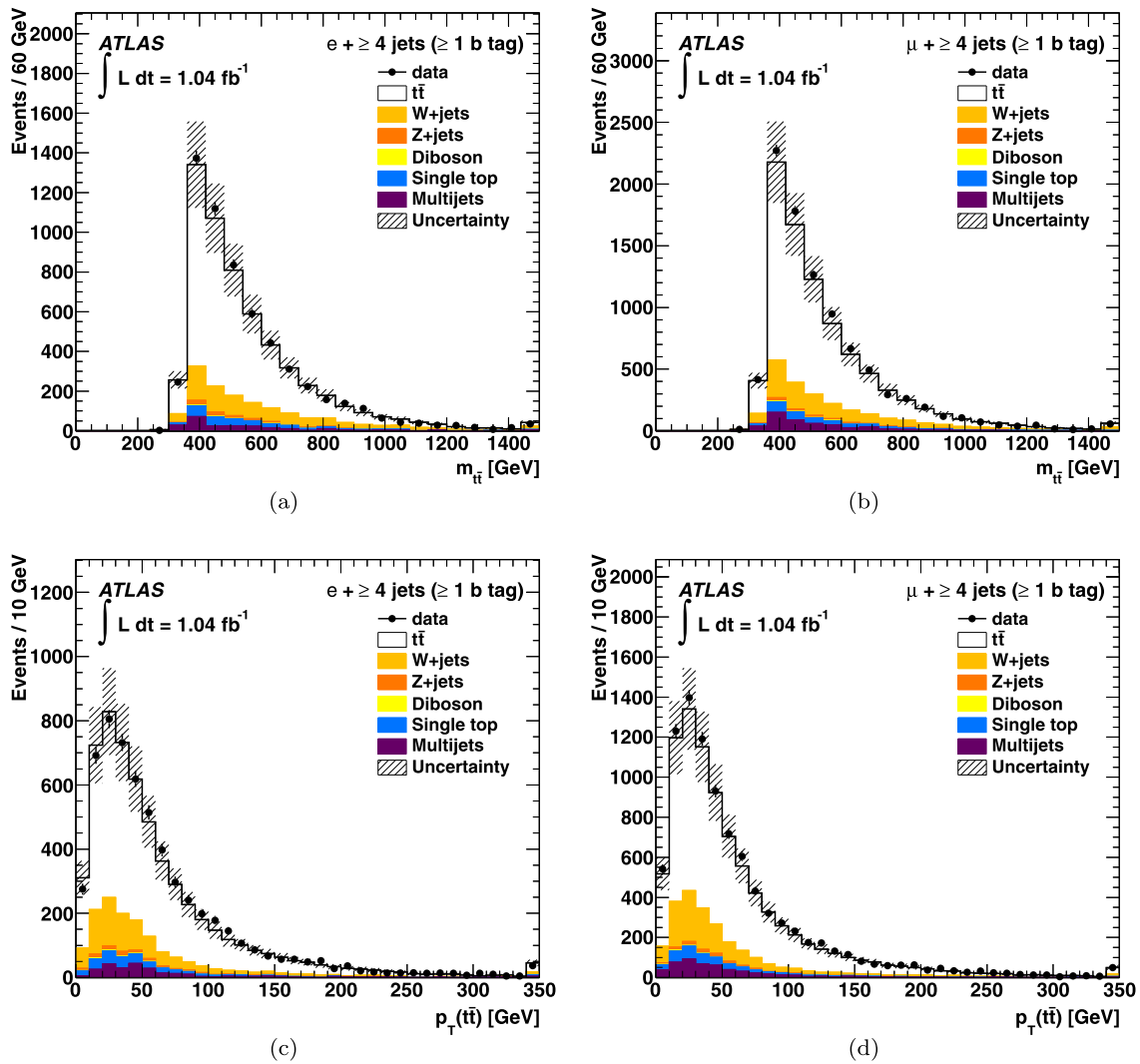


Fig. 1 Expected and observed distributions for the invariant mass (plots (a) and (b)) and transverse momentum (plots (c) and (d)) of the reconstructed $t\bar{t}$ system. The *left hand panels* show distributions in the electron channel, while the *right hand panels* show distributions in the muon channel. The data are compared to the sum of the $t\bar{t}$ signal contribution and backgrounds. The background contributions from

$W +$ jets and multijet production have been estimated from data, while the other backgrounds are estimated from simulation. The uncertainty on the combined signal and background estimate includes systematic contributions. Overflows are shown in the highest bin of each histogram

The likelihood is computed as

$$\begin{aligned}
 L = & \mathcal{B}(\tilde{E}_{p,1}, \tilde{E}_{p,2} | m_W, \Gamma_W) \cdot \mathcal{B}(\tilde{E}_{lep}, \tilde{E}_v | m_W, \Gamma_W) \\
 & \cdot \mathcal{B}(\tilde{E}_{p,1}, \tilde{E}_{p,2}, \tilde{E}_{p,3} | m_t, \Gamma_t) \cdot \mathcal{B}(\tilde{E}_{lep}, \tilde{E}_v, \tilde{E}_{p,4} | m_t, \Gamma_t) \\
 & \cdot \mathcal{W}(\hat{E}_x^{miss} | \tilde{p}_{x,v}) \cdot \mathcal{W}(\hat{E}_y^{miss} | \tilde{p}_{y,v}) \cdot \mathcal{W}(\hat{E}_{lep} | \tilde{E}_{lep}) \\
 & \cdot \prod_{i=1}^4 \mathcal{W}(\hat{E}_{jet,i} | \tilde{E}_{p,i}) \\
 & \cdot \prod_{i=1}^4 P(\text{tagged} | \text{parton flavour}), \tag{4}
 \end{aligned}$$

where:

- Symbols \mathcal{B} represent Breit-Wigner functions, evaluated using invariant masses of sums of appropriate parton and lepton four-vectors. The pole masses of the W boson and the top quark are fixed to $m_W = 80.4$ GeV and $m_t = 172.5$ GeV, respectively. Their widths are taken to be $\Gamma_W = 2.1$ GeV and $\Gamma_t = 1.5$ GeV.
- Symbols \mathcal{W} represent the transfer functions associating the reconstructed quantities (\hat{X}) to quarks and leptons produced in the hard scattering (\tilde{X}). $\tilde{E}_{p,i}$ are the energies of partons associated to jets with measured energies $\hat{E}_{jet,i}$. These transfer functions are derived from Monte Carlo simulation.

– $P(\text{tagged} | \text{parton flavour})$ is the b -tagging probability or rejection efficiency, depending on the parton flavour, as obtained from Monte Carlo simulation.

The likelihood is maximised with respect to the energies of the partons, the energy of the charged lepton, and the components of the neutrino three-momentum. The assignment of jets to partons which gives the highest likelihood value is selected. Finally, the sign of the charge of the top quark (or anti-quark) decaying into the lepton is determined from the lepton charge.

The overall efficiency for the reconstruction of the correct event topology is found to be 74 % in Monte Carlo simulated $t\bar{t}$ events. Only those events where four jets and a lepton are matched to partonic particles are considered for the efficiency computation.

Distributions of the invariant mass and transverse momentum of the reconstructed top-antitop pair are shown in Fig. 1.

7 Unfolding

The measured distributions of top and anti-top rapidities are distorted by detector effects and an event selection bias. To correct for these distortions the experimental distributions are unfolded to the four-vectors of the top quarks before decay.

The relation between a true distribution T_j (assuming, for simplicity, that there is only one observable of interest) and the reconstructed distribution S_i after detector simula-

tion and event selection can be written as:

$$S_i = \sum_j R_{ij} T_j, \tag{5}$$

where R_{ij} is the response matrix defined as the probability to observe an event in bin i when it is expected in bin j .

The true distribution T_j can be obtained from the observed distribution S_i by inverting the response matrix. The unfolding problem can similarly be formulated for the case of multiple observables. In this analysis, Bayes' theorem is applied iteratively in order to perform the unfolding [39].

The unfolding is performed using response matrices which account for both detector response and acceptance effects. The response matrices are calculated using Monte Carlo events generated with MC@NLO. The unfolding is done separately, after background subtraction, for the inclusive measured distribution of $\Delta|y|$ (a one-dimensional unfolding problem), and the measured distribution $\Delta|y|$ as a function of the reconstructed top-antitop invariant mass $m_{t\bar{t}}$ (a two-dimensional unfolding problem).

Two bins are used for $m_{t\bar{t}}$ in the two-dimensional unfolding of $\Delta|y|$ versus $m_{t\bar{t}}$, separated at $m_{t\bar{t}} = 450$ GeV. The choice of this $m_{t\bar{t}}$ value is motivated by the observed CDF forward-backward asymmetry [6] and by separating the data sample into two bins with roughly equal number of events.

An additional cut on the value of the likelihood for the $t\bar{t}$ candidate is required in the two-dimensional unfolding, since a large fraction of simulated events with a badly reconstructed $m_{t\bar{t}}$ are found to have a low likelihood value.

The response matrix (including both detector and acceptance effects) for the inclusive A_C measurement is shown in Fig. 2. Six bins in $\Delta|y|$, in the range $-3 < \Delta|y| < 3$,

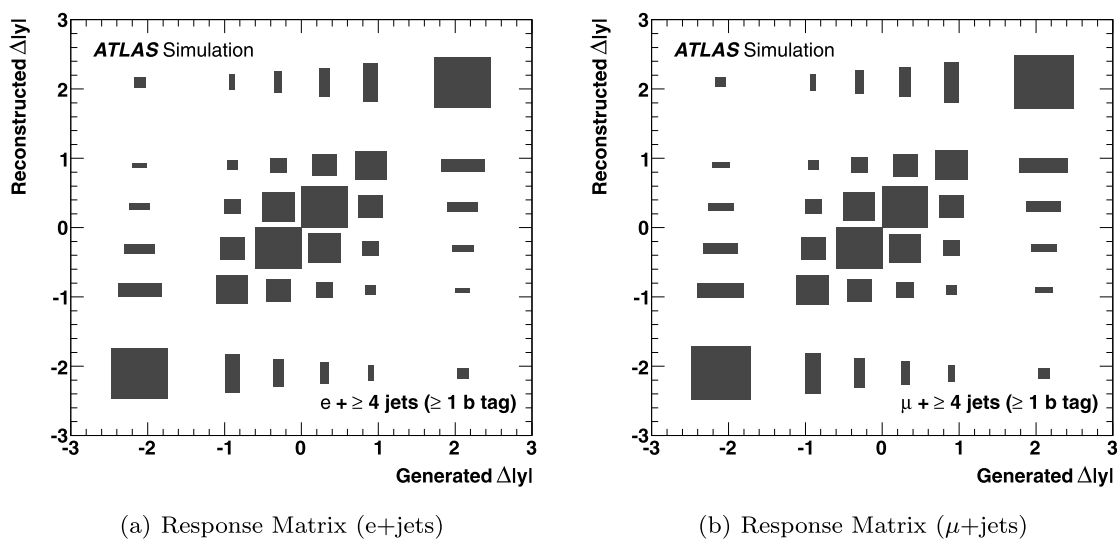


Fig. 2 Correlations between the true and reconstructed values of $\Delta|y|$ encoded in the unfolding response matrix for the electron (left) and muon (right) channels. The value of an entry in the matrix is proportional to the area of the corresponding box

are used in the response matrix, with the outermost bins broader than the inner bins in order to avoid the occurrence of bins with no entries in the measured distributions. Only a very small fraction of simulated $t\bar{t}$ events are found to have $|\Delta|y| > 3$, and hence such events have a negligible influence on the results.

The unfolding procedure is applied to the observed $\Delta|y|$ distribution in data, after subtracting background contributions. When performing the background subtraction, the shape of the multijet background is obtained by applying the Matrix Method (described in Sect. 5.1) in bins of $\Delta|y|$. The shape of all remaining backgrounds is taken from Monte Carlo simulation. The value of A_C after unfolding is obtained by counting the numbers of events with $\Delta|y| > 0$ and $\Delta|y| < 0$ in the unfolded $\Delta|y|$ distribution.

8 Systematic uncertainties

Several sources of systematic uncertainties are taken into account in this analysis. These are categorised into the detector modelling, the modelling of signal and background processes and the unfolding method.

8.1 Detector modelling

Small mis-modellings of muon or electron trigger, reconstruction and selection efficiencies in simulation are corrected for by scale factors derived from measurements of the efficiency in data. $Z \rightarrow \mu\mu$ or $Z \rightarrow ee$ and $W \rightarrow e\nu$ decays are used to obtain scale factors as functions of the lepton kinematics. The uncertainties are evaluated by varying the lepton and signal selections and from the uncertainty in the evaluation of the backgrounds. Systematic uncertainties at the level of 1 % are found for both cases. The same processes are used to measure the lepton momentum scale and resolution. Scale factors, with uncertainties at the level of (1–1.5) %, are derived to match the simulation to observed distributions. A systematic uncertainty for charge mis-identification of leptons is assigned which is negligible for muons and ranges from 0.2 % to 3 % for electrons depending on $|\eta|$.

The jet energy scale is derived using information from test-beam data, collision data and simulation. Its uncertainty varies between 2.5 % and 8 % in the central region, depending on jet p_T and η [33]. This includes uncertainties in the flavour composition of the sample and mis-measurements due to the effect of nearby jets. Pile-up gives additional uncertainties of up to 5 % (7 %) in the central (forward) region. An extra uncertainty of 0.8 % to 2.5 %, depending on jet p_T , is assigned to jets arising from the fragmentation of b -quarks, due to differences between light and gluon jets as opposed to jets containing b -hadrons. The jet energy resolution and reconstruction efficiency are measured in data using

techniques described in Refs. [33, 40], and their uncertainties are found to be 10 % and (1–2) %, respectively.

The b -tagging efficiencies and mis-tag rates are measured in data. Jet p_T dependent scale factors, applied to simulations to match the efficiencies measured in data, have uncertainties which range from 9 % to 15 % and 11 % to 22 %, respectively. A systematic uncertainty is assigned for a potential difference of up to 5 % between the b -tagging efficiency for b -jets and that of \bar{b} -jets. The uncertainty on the measured luminosity is 3.7 % [41, 42].

Due to a hardware failure, later repaired, one small region of the liquid argon calorimeter could not be read out in a subset of the data corresponding to 84 % of the total integrated luminosity. Data events in which an electron or jet with $p_T > 20$ GeV is close to the affected calorimeter region are rejected for the relevant part of the dataset. Monte Carlo simulated events with electrons or jets of $p_T > 20$ GeV close to the affected region are rejected with a probability equal to the fraction of the integrated luminosity of data for which the calorimeter hardware problem was present. A systematic uncertainty is evaluated by varying the p_T -threshold in data of the electrons and jets near the affected region by ± 4 GeV, corresponding to the uncertainty in the energy lost by objects in the affected region.

8.2 Signal and background modelling

The systematic uncertainty in the modelling of the signal process is assessed by simulations based on different Monte Carlo generators. Sources of systematic uncertainty considered here are the choice of generator and parton shower model, the choice of parton density functions, the assumed top quark mass and the choice of parameters which control the amount of initial and final state radiation. Predictions from the MC@NLO and POWHEG [43, 44] generators are compared. The parton showering is tested by comparing two POWHEG samples interfaced to HERWIG and PYTHIA, respectively. The amount of initial and final state radiation is varied by modifying parameters in ACERMC [45] interfaced to PYTHIA according to Ref. [46]. The parameters are varied in a range comparable to those used in the Perugia Soft/Hard tune variations [47]. The impact of the choice of parton density functions is studied using the procedure described in Ref. [48]. MC@NLO samples are generated assuming different top quark masses and their predictions are compared. The observed differences in the results are scaled to variations of ± 0.9 GeV according to the uncertainty on the measured value [49].

As described in Sect. 5, background processes are either modelled by simulation or estimated in auxiliary measurements. The uncertainty in the estimate of the multijet background is evaluated by considering modified definitions of the loose data sample, taking into account the statistical uncertainty in measurements of ϵ_{real} , ϵ_{fake} described in

Sect. 5.1 as well as the uncertainties in the normalisations of the $W + \text{jets}$ and $Z + \text{jets}$ backgrounds which are subtracted in the control region. The total uncertainty is estimated to be 100 %. The normalisation of $W + \text{jets}$ processes is evaluated from auxiliary measurements using the asymmetric production of positively and negatively charged W bosons in $W + \text{jets}$ events. The uncertainty is estimated to be 21 % and 23 % in the four jet bin, for the electron and muon channels respectively. This uncertainty was estimated by evaluating the effect on both r_{MC} and $k_{2 \rightarrow \geq 4}$ from the JES uncertainty and different PDF and generator choices. Systematic uncertainties on the shape of $W + \text{jets}$ distributions are assigned based on differences in simulated events generated with different simulation parameters. Scaling factors correcting the fraction of heavy flavour contributions in simulated $W + \text{jets}$ samples are estimated in auxiliary measurements, as described in Sect. 5.2. The systematic uncertainties are found by changing the normalisations of the non- W processes within their uncertainties when computing $W_{i,\text{pretag}}^{\text{Data}}$, $W_{i,\text{tagged}}^{\text{Data}}$, as well as taking into account the impact of uncertainties in b -tagging efficiencies. The total uncertainties are 47 % for $Wb\bar{b} + \text{jets}$ and

$Wc\bar{c} + \text{jets}$ contributions and 32 % for $Wc + \text{jets}$ contributions. The normalisation of $Z + \text{jet}$ events is estimated using Berends–Giele-scaling [50]. The uncertainty in the normalisation is 48 % in the four jet bin and increases with the jet multiplicity. A systematic uncertainty in the shape is accounted for by comparing simulated samples generated with ALPGEN and SHERPA [51]. The uncertainty on the normalisation of the small background contributions from single top and diboson production is estimated to be about 10 % (depending on the channel) and 5 %, respectively.

Limited Monte Carlo sample sizes give rise to a systematic uncertainty in the response matrix. This is accounted for by independently varying the bins of the response matrix according to Poisson distributions.

8.3 Uncertainties from unfolding

Closure tests are performed in order to check the validity of the unfolding procedure. Reweighted $t\bar{t}$ samples with different amounts of asymmetry are considered. Pseudoexperiments are performed, varying the entries in histograms of

Table 2 List of sources of systematic uncertainties and their impact on the measured asymmetry in the electron and muon channel. In cases where asymmetric uncertainties were obtained, a symmetrisation of the uncertainties was performed by taking the average of the absolute deviations under systematic shifts from the nominal value

Source of systematic uncertainty on A_C	Electron channel	Muon channel
<i>Detector modelling</i>		
Jet energy scale	0.012	0.006
Jet efficiency and resolution	0.001	0.007
Muon efficiency and resolution	<0.001	0.001
Electron efficiency and resolution	0.003	0.001
b-Tag scale factors	0.004	0.002
Calorimeter readout	0.001	0.004
Charge mis-ID	<0.001	<0.001
b-Tag charge	0.001	0.001
<i>Signal and background modelling</i>		
Parton shower/fragmentation	0.010	0.010
Top mass	0.007	0.007
$t\bar{t}$ modelling	0.011	0.011
ISR and FSR	0.010	0.010
PDF	<0.001	<0.001
$W + \text{jets}$ normalisation and shape	0.008	0.005
$Z + \text{jets}$ normalisation and shape	0.005	0.001
Multijet background	0.011	0.001
Single top	<0.001	<0.001
Diboson	<0.001	<0.001
MC statistics	0.006	0.005
Unfolding convergence	0.005	0.007
Unfolding bias	0.004	<0.001
Luminosity	0.001	0.001
Total systematic uncertainty	0.028	0.024

the reconstructed distribution, to confirm that the response of the unfolding is linear in the true value of A_C and that the true value of A_C is recovered on average. A total of 40 iterations are used in both channels for the inclusive A_C measurement. For the measurement of A_C as a function of $m_{\bar{t}t}$, 80 iterations are used. The number of iterations is chosen by ensuring that the unfolding procedure has converged in the sense that the absolute change in the unfolded value of A_C after performing an extra iteration is less than 0.001. It is found that the unfolded values of A_C from all pseudoexperiments and the data converge before the chosen numbers of iterations. The potential bias arising from the choice of convergence criterion is taken into account by adding an additional systematic uncertainty corresponding to the change in the unfolded value of A_C obtained by further increasing the number of iterations to very large values (10^5).

Pull distributions are constructed from pseudoexperiments and a relative shift of between 0 % and 10 % is found in the unfolded value of A_C with respect to the true value. An extra systematic uncertainty is assigned to the unfolded value of A_C obtained from data, corresponding to this shift.

In pseudoexperiments, a small bias is observed in the unfolded distributions corresponding to a relative difference of a few percent between the unfolded result and true value in each bin. An additional relative uncertainty of (2–5) % is applied to all bins of the unfolded distributions, corresponding to the largest relative bin deviation observed in pseudoexperiments.

The statistical uncertainty in the unfolded measurement was computed using pseudoexperiments, propagating the uncertainties from the measured distribution using the statistical correlation matrix.

8.4 Impact of systematic uncertainties

The impact of the systematic uncertainties is evaluated by modifying the subtracted background before unfolding and by modifying the response matrix used for unfolding when relevant. In particular the detector modelling systematic uncertainties are evaluated by shifting the estimated background as well as modifying the response matrix. Signal modelling uncertainties are computed by replacing the response matrix, and background modelling uncertainties by modifying the estimated background.

Table 2 summarises the sources of systematic uncertainties for the inclusive measurement of the charge asymmetry, and their impact on the measured asymmetry, after unfolding. The systematics for the two $m_{\bar{t}t}$ bins are determined in a similar fashion. The evaluation of some systematic uncertainties is limited by the finite size of the Monte Carlo samples. In these cases, the larger of the electron and muon channel uncertainties is used for the uncertainty on the combined result. The resulting combined systematic uncertainties are ± 0.028 in the electron channel and ± 0.024 in the muon channel.

9 Summary of results

The measured distributions of the top-antitop rapidity difference $\Delta|y| = |y_t| - |y_{\bar{t}}|$ before unfolding are shown in Fig. 3 for the electron and muon channel. Figure 4 shows the corresponding $\Delta|y|$ distributions after unfolding. After unfolding, the bins of the measured distribution have statistical and systematic correlations. Adjacent bins of the $\Delta|y|$ distributions are found to be statistically anti-correlated with neg-

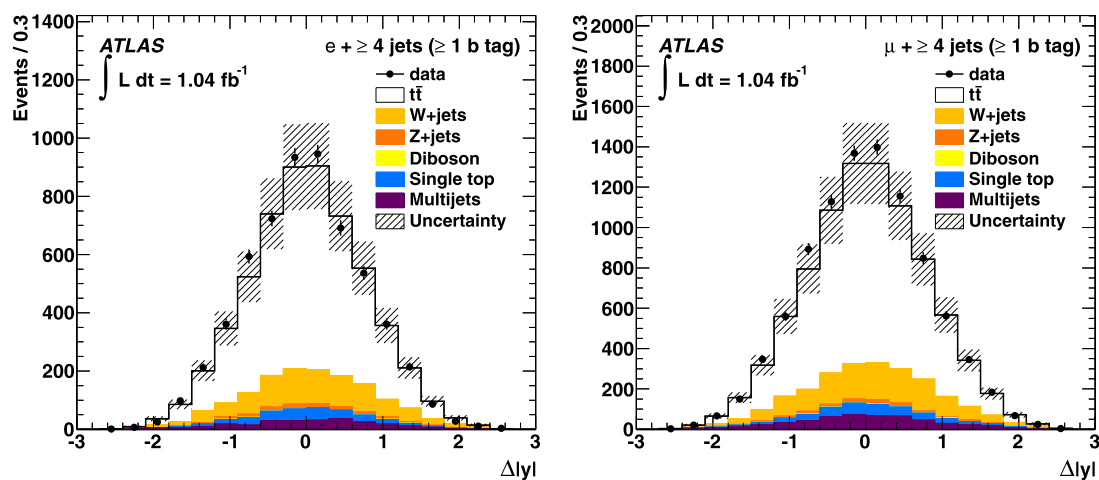


Fig. 3 The measured $\Delta|y|$ distribution before unfolding for the electron channel (*left*) and for the muon channel (*right*) after b -tagging is applied. Data (*points*) and Monte Carlo estimates (*solid lines*) are represented. The multijet background and the normalisation of the

$W + \text{jets}$ background are obtained as explained in Sect. 5. The uncertainty on the combined signal and background estimate includes both statistical and systematic contributions

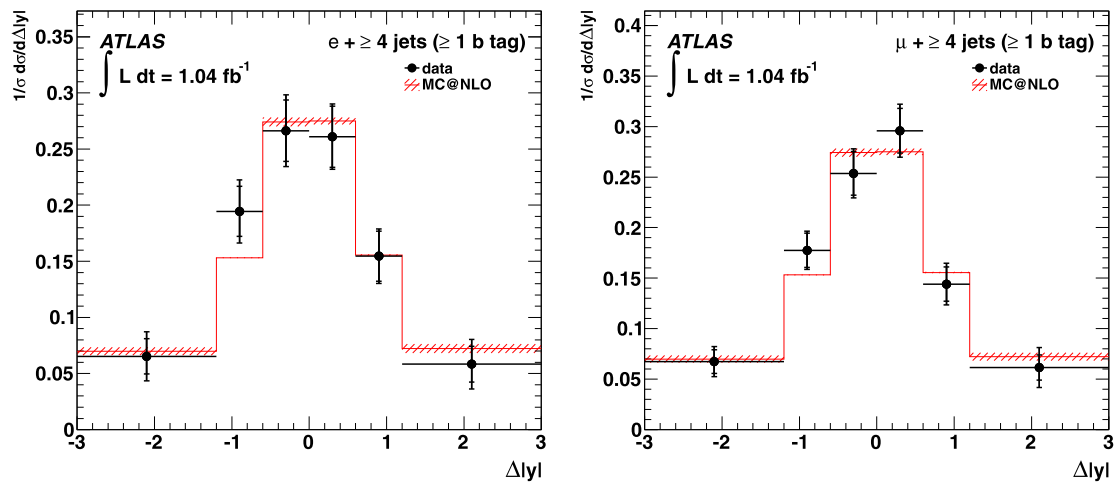


Fig. 4 The unfolded $\Delta|y|$ distribution for the electron channel (*left*) and the muon channel (*right*) after b -tagging, compared to the prediction from MC@NLO. The uncertainties on the measurement include both statistical and systematic contributions, which are shown separately. The inner part of the error bars corresponds to the statistical

component of the uncertainty, while the outer part corresponds to the systematic component. The error bands on the MC@NLO prediction include uncertainties from parton distribution functions and renormalisation and factorisation scales

Table 3 The measured inclusive charge asymmetry values for the electron and muon channels after background subtraction, before and after unfolding

Asymmetry	Reconstructed	Detector and acceptance unfolded
A_C (electron)	-0.034 ± 0.019 (stat.) ± 0.010 (syst.)	-0.047 ± 0.045 (stat.) ± 0.028 (syst.)
A_C (muon)	-0.010 ± 0.015 (stat.) ± 0.008 (syst.)	-0.002 ± 0.036 (stat.) ± 0.024 (syst.)
Combined		-0.019 ± 0.028 (stat.) ± 0.024 (syst.)

ative correlation coefficients of up to -0.6 , whereas other correlations are small.

The measured values of the top charge asymmetry before and after unfolding, defined by (1) in terms of $\Delta|y|$, are summarised in Table 3. The analytic best linear unbiased estimator (BLUE) method [52, 53] is used to combine the measurement in the electron and muon channels after correction for detector resolution and acceptance.

The measured asymmetries are:

$$A_C = -0.019 \pm 0.028 \text{ (stat.)} \pm 0.024 \text{ (syst.)}$$

for the integrated sample, and

$$A_C = -0.052 \pm 0.070 \text{ (stat.)} \pm 0.054 \text{ (syst)}$$

for $m_{t\bar{t}} < 450$ GeV,

$$A_C = -0.008 \pm 0.035 \text{ (stat.)} \pm 0.032 \text{ (syst)}$$

for $m_{t\bar{t}} > 450$ GeV.

The measurement for the integrated sample can be compared with the result of the CMS Collaboration, $A_C = -0.013 \pm 0.028$ (stat) $^{+0.029}_{-0.031}$ (syst) [19]. Figure 5 summarises the measurements for the two $m_{t\bar{t}}$ regions. These results are compatible with the prediction from the MC@NLO Monte Carlo

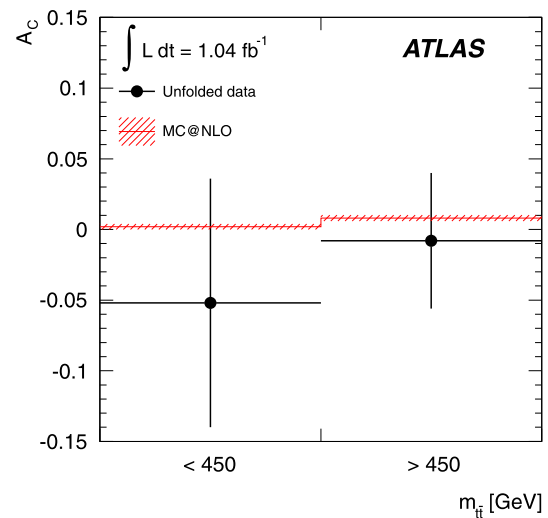


Fig. 5 Unfolded asymmetries in two regions of $m_{t\bar{t}}$ compared to the prediction from MC@NLO. The error bands on the MC@NLO prediction include uncertainties from parton distribution functions and renormalisation and factorisation scales

generator of $A_C = 0.006 \pm 0.002$,⁵ showing no evidence for an enhancement from physics beyond the Standard Model.

⁵The prediction of 0.0115 ± 0.0006 for the charge asymmetry found in Ref. [54] differs from the MC@NLO prediction of 0.006 ± 0.002 , due

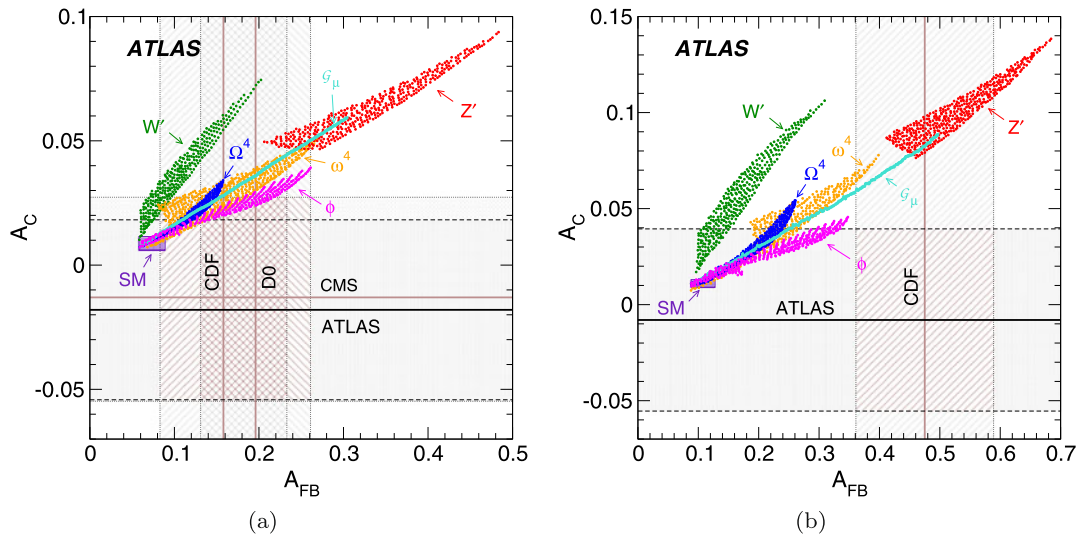


Fig. 6 Measured forward–backward asymmetries from the Tevatron and charge asymmetries from the LHC, compared to predictions from the SM as well as predictions incorporating various potential new physics contributions. The horizontal (vertical) bands and lines cor-

respond to the ATLAS and CMS (CDF and D0) measurements. In (a) the inclusive values are presented and in (b) the ATLAS measurement for $m_{t\bar{t}} > 450$ GeV is compared to the CDF measurement. The MC predictions for the new physics models are from Refs. [17, 55]

10 Comparison of LHC and Tevatron results

The measurement of the charge asymmetry at the LHC is a test of the unexpectedly large forward–backward asymmetry observed at the Tevatron. However, because the LHC is a pp collider and the centre of mass energy is around three times larger, any relation between the two asymmetries is model-dependent. Here a comparison is made between the predicted values of the Tevatron and LHC asymmetries for a few simple models beyond the SM. These are: (i) a flavour-changing Z' boson with right-handed couplings, exchanged in the t channel in $u\bar{u} \rightarrow t\bar{t}$ [10]; (ii) a W' boson, also with right-handed couplings, contributing in $d\bar{d} \rightarrow t\bar{t}$ [11]; a heavy axigluon G_μ exchanged in the s channel [8, 9]; (iv) a scalar doublet ϕ , with the same quantum numbers as the SM Higgs [55]; (v) a charge 4/3 scalar, colour-sextet (Ω^4) or colour-triplet (ω^4), contributing in the u channel to $u\bar{u} \rightarrow t\bar{t}$ [12, 13]. In all these models, the parameter space is described by the mass M of the new particle (except for the axigluon which is assumed to be heavy, with $M \gg 7$ TeV) and a single coupling g .

In order to find the correlated predictions for the forward–backward and charge asymmetries in each model, a comprehensive scan over the mass M and the coupling g is performed using the PROTOS generator [56], considering masses between 100 GeV and 10 TeV and the range of couplings for which the new physics contribution to the $t\bar{t}$ cross

section at the Tevatron lies in the interval $[-0.8, 1.7]$ pb. This is a conservative requirement which takes into account the different predictions for the SM cross section as well as the experimental measurement (see Ref. [17] for details).

In addition, a conservative upper limit on new physics contributions to $\sigma_{t\bar{t}}$ for $m_{t\bar{t}} > 1$ TeV is imposed. Further details can be found in Refs. [17, 55]. The coloured areas in Fig. 6(a) represent the ranges of predicted values for the inclusive Tevatron forward–backward asymmetry, A_{FB} , and the inclusive LHC charge asymmetry, A_C , for the new physics models. The new physics contributions are computed using the tree-level SM amplitude plus the one(s) from the new particle(s). To a good approximation, the total asymmetries A_{FB} , A_C are obtained from the former by summing the SM contribution (at NLO in the lowest order). The horizontal lines correspond to the present ATLAS measurement and the measurement reported by the CMS Collaboration [19]. The vertical lines correspond to the asymmetry measurements at the Tevatron, $A_{FB} = 0.158 \pm 0.075$ [6] and $A_{FB} = 0.196 \pm 0.065$ [7].

The ATLAS charge asymmetry measurement disfavors models with a new flavour-changing Z' or W' vector boson proposed to explain the measured Tevatron asymmetry. Minimal Z' models are also excluded by the non-observation of same-sign top quark production [57]. For the other new physics models the asymmetries measured at the Tevatron are consistent with this measurement, within the experimental uncertainties.

Figure 6(b) shows the allowed regions for the high-mass asymmetries ($m_{t\bar{t}} > 450$ GeV) at the Tevatron and the LHC for the six new physics models. The vertical lines represent

to the former taking the LO prediction for the denominator in the definition (1) of A_C , and taking into account QED effects. The uncertainty on the MC@NLO prediction is obtained by considering variations in the renormalisation and factorisation scales and different sets of PDFs.

the CDF measurement $A_{FB} = 0.475 \pm 0.114$ [6], while the horizontal lines correspond to the present ATLAS measurement. In both panels of Fig. 6, the range of variation of SM predictions found in Refs. [54, 58, 59] is indicated by a box. The predictions of the six new physics models are in tension with the CDF and ATLAS high-mass measurements considered together.

11 Conclusion

To summarise, the top quark charge asymmetry was measured in $t\bar{t}$ events with a single lepton (electron or muon), at least four jets and large missing transverse momentum using an integrated luminosity of 1.04 fb^{-1} recorded by the ATLAS experiment at a centre of mass energy of $\sqrt{s} = 7 \text{ TeV}$. The reconstruction of $t\bar{t}$ events was performed using a kinematic fit. The reconstructed inclusive distribution of $\Delta|y|$ and the distribution as a function of $m_{t\bar{t}}$ were unfolded after background subtraction to obtain results that can be directly compared with theoretical computations. The results are compatible with the prediction from the MC@NLO Monte Carlo generator. These measurements disfavour models with a new flavour-changing Z' or W' vector boson that have been suggested to explain the measured Tevatron asymmetry.

Acknowledgements We thank CERN for the very successful operation of the LHC, as well as the support staff from our institutions without whom ATLAS could not be operated efficiently.

We acknowledge the support of ANPCyT, Argentina; YerPhI, Armenia; ARC, Australia; BMWF, Austria; ANAS, Azerbaijan; SSTC, Belarus; CNPq and FAPESP, Brazil; NSERC, NRC and CFI, Canada; CERN; CONICYT, Chile; CAS, MOST and NSFC, China; COLCIENCIAS, Colombia; MSMT CR, MPO CR and VSC CR, Czech Republic; DNRF, DNSRC and Lundbeck Foundation, Denmark; EPLANET and ERC, European Union; IN2P3-CNRS, CEA-DSM/IRFU, France; GNAS, Georgia; BMBF, DFG, HGF, MPG and AvH Foundation, Germany; GSRT, Greece; ISF, MINERVA, GIF, DIP and Benoziyo Center, Israel; INFN, Italy; MEXT and JSPS, Japan; CNRST, Morocco; FOM and NWO, Netherlands; RCN, Norway; MNiSW, Poland; GRICES and FCT, Portugal; MERYS (MECTS), Romania; MES of Russia and ROSATOM, Russian Federation; JINR; MSTD, Serbia; MSSR, Slovakia; ARRS and MVZT, Slovenia; DST/NRF, South Africa; MICINN, Spain; SRC and Wallenberg Foundation, Sweden; SER, SNSF and Cantons of Bern and Geneva, Switzerland; NSC, Taiwan; TAEK, Turkey; STFC, the Royal Society and Leverhulme Trust, United Kingdom; DOE and NSF, United States of America.

The crucial computing support from all WLCG partners is acknowledged gratefully, in particular from CERN and the ATLAS Tier-1 facilities at TRIUMF (Canada), NDGF (Denmark, Norway, Sweden), CC-IN2P3 (France), KIT/GridKA (Germany), INFN-CNAF (Italy), NL-T1 (Netherlands), PIC (Spain), ASGC (Taiwan), RAL (UK) and BNL (USA) and in the Tier-2 facilities worldwide.

Open Access This article is distributed under the terms of the Creative Commons Attribution License which permits any use, distribution, and reproduction in any medium, provided the original author(s) and the source are credited.

References

1. S. Jung, A. Pierce, J.D. Wells, Top quark asymmetry from a non-Abelian horizontal symmetry. *Phys. Rev. D* **83**, 114039 (2011). [arXiv:1103.4835](#) [hep-ph]
2. R. Diener, S. Godfrey, T.A.W. Martin, Using final state pseudorapidities to improve s-channel resonance observables at the LHC. *Phys. Rev. D* **80**, 075014 (2009). [arXiv:0909.2022](#) [hep-ph]
3. J.H. Kühn, G. Rodrigo, Charge asymmetry in hadroproduction of heavy quarks. *Phys. Rev. Lett.* **81**, 49–52 (1998). [arXiv:hep-ph/9802268](#)
4. V.M. Abazov et al. (D0 Collaboration), Measurements of the forward-backward charge asymmetry in top-quark pair production. *Phys. Rev. Lett.* **100**, 142002 (2008). [arXiv:0712.0851](#) [hep-ex]
5. T. Aaltonen et al. (CDF Collaboration), Forward–backward asymmetry in top quark pair production in $p\bar{p}$ collisions at $\sqrt{s} = 1.96 \text{ TeV}$. *Phys. Rev. Lett.* **101**, 202001 (2008). [arXiv:0806.2472](#) [hep-ex]
6. T. Aaltonen et al. (CDF Collaboration), Evidence for a mass dependent forward–backward asymmetry in top quark pair production. *Phys. Rev. D* **83**, 112003 (2011). [arXiv:1101.0034](#) [hep-ex]
7. V.M. Abazov et al. (D0 Collaboration), Forward-backward asymmetry in top quark–antiquark production. *Phys. Rev. D* **84**, 112005 (2011). [arXiv:1107.4995](#) [hep-ex]
8. P. Ferrario, G. Rodrigo, Constraining heavy colored resonances from top-antitop quark events. *Phys. Rev. D* **80**, 051701 (2009). [arXiv:0906.5541](#) [hep-ph]
9. P.H. Frampton, J. Shu, K. Wang, Axigluon as possible explanation for $p\bar{p} \rightarrow t\bar{t}$ forward–backward asymmetry. *Phys. Lett. B* **683**, 294–297 (2010). [arXiv:0911.2955](#) [hep-ph]
10. S. Jung, H. Murayama, A. Pierce, J.D. Wells, Top quark forward–backward asymmetry from new t-channel physics. *Phys. Rev. D* **81**, 015004 (2010). [arXiv:0907.4112](#) [hep-ph]
11. K. Cheung, W.-Y. Keung, T.-C. Yuan, Top quark forward–backward asymmetry. *Phys. Lett. B* **682** (2009). [arXiv:0908.2589](#) [hep-ph]
12. J. Shu, T.M. Tait, K. Wang, Explorations of the top quark forward–backward asymmetry at the Tevatron. *Phys. Rev. D* **81**, 034012 (2010). [arXiv:0911.3237](#) [hep-ph]
13. I. Dorsner, S. Fajfer, J.F. Kamenik, N. Kosnik, Light colored scalars from grand unification and the forward–backward asymmetry in top quark pair production. *Phys. Rev. D* **81**, 055009 (2010). [arXiv:0912.0972](#) [hep-ph]
14. B. Grinstein, A.L. Kagan, M. Trott, J. Zupan, Forward–backward asymmetry in $t\bar{t}$ production from flavour symmetries. *Phys. Rev. Lett.* **107**, 012002 (2011). [arXiv:1102.3374](#) [hep-ph]
15. Z. Ligeti, G.M. Tavares, M. Schmaltz, Explaining the $t\bar{t}$ forward–backward asymmetry without dijet or flavor anomalies. *J. High Energy Phys.* **06**, 109 (2011). [arXiv:1103.2757](#) [hep-ph]
16. J.A. Aguilar-Saavedra, M. Perez-Victoria, Probing the Tevatron $t\bar{t}$ asymmetry at LHC. *J. High Energy Phys.* **05**, 034 (2011). [arXiv:1103.2765](#) [hep-ph]
17. J. Aguilar-Saavedra, M. Perez-Victoria, Asymmetries in $t\bar{t}$ production: LHC versus Tevatron. *Phys. Rev. D* **84**, 115013 (2011). [arXiv:1105.4606](#) [hep-ph]
18. J. Aguilar-Saavedra, M. Perez-Victoria, Shaping the top asymmetry. *Phys. Lett. B* **705**, 228 (2011). [arXiv:1107.2120](#) [hep-ph]
19. CMS Collaboration, Measurement of the charge asymmetry in top-quark pair production in proton–proton collisions at $\sqrt{s} = 7 \text{ TeV}$. *Phys. Lett. B* **709**, 28 (2012). [arXiv:1112.5100](#) [hep-ex]
20. ATLAS Collaboration, The ATLAS experiment at the CERN large hadron collider. *J. Instrum.* **3**, S08003 (2008)
21. S. Frixione, B.R. Webber, Matching NLO QCD computations and parton shower simulations. *J. High Energy Phys.* **0206**, 029 (2002). [hep-ph/0204244](#)

22. P.M. Nadolsky et al., Implications of CTEQ global analysis for collider observables. *Phys. Rev. D* **78**, 013004 (2008). [arXiv:0802.0007](#) [hep-ph]
23. G. Corcella et al., HERWIG 6: an event generator for hadron emission reactions with interfering gluons (including supersymmetric processes). *J. High Energy Phys.* **0101**, 010 (2001). [hep-ph/0011363](#)
24. J.M. Butterworth, J.R. Forshaw, M.H. Seymour, Multiparton interactions in photoproduction at HERA. *Z. Phys. C* **72**, 637–646 (1996). [arXiv:hep-ph/9601371](#)
25. M. Aliev et al., HATHOR: HAdronic Top and Heavy quarks crOss section calculator. *Comput. Phys. Commun.* **182**, 1034–1046 (2011). [arXiv:1007.1327](#) [hep-ph]
26. M.L. Mangano et al., ALPGEN, a generator for hard multiparton processes in hadronic collisions. *J. High Energy Phys.* **0307**, 001 (2003). [hep-ex/0206293](#)
27. J. Pumplin, et al., New generation of parton distributions with uncertainties from global QCD analysis. *J. High Energy Phys.* **07**, 012 (2002). [arXiv:hep-ph/0201195](#)
28. A. Sherstnev, R. Thorne, Parton distributions for LO generators. *Eur. Phys. J. C* **55**, 553–575 (2008). [arXiv:0711.2473](#) [hep-ph]
29. S. Agostinelli et al., Geant4 a simulation toolkit. *Nucl. Instrum. Methods A* **506**, 250 (2003)
30. ATLAS Collaboration, The ATLAS simulation infrastructure. *Eur. Phys. J. C Part. Fields* **70**, 823–874 (2010)
31. ATLAS Collaboration, Electron performance measurements with the ATLAS detector using the 2010 LHC proton–proton collision data. *Eur. Phys. J. C* **72**, 1909 (2012). [arXiv:1110.3174](#) [hep-ex]
32. M. Cacciari, G.P. Salam, G. Soyez, The anti-k(t) jet clustering algorithm. *J. High Energy Phys.* **0804**, 063 (2008). [arXiv:0802.1189](#) [hep-ph]
33. ATLAS Collaboration, Jet energy measurement with the ATLAS detector in proton–proton collisions at $\sqrt{s} = 7$ TeV. [arXiv:1112.6426](#) [hep-ex]
34. ATLAS Collaboration, Performance of missing transverse momentum reconstruction in proton–proton collisions at 7 TeV with ATLAS. *Eur. Phys. J. C* **72**, 2012 (1844). [arXiv:1108.5602](#) [hep-ex]
35. R.E. Kalman, A new approach to linear filtering and prediction problems. *J. Basic Eng., Ser. D* **82**, 35–45 (1960)
36. ATLAS Collaboration, Measurement of the top quark-pair production cross section with ATLAS in pp collisions at $\sqrt{s} = 7$ TeV. *Eur. Phys. J. C* **71**, 1577 (2011). [arXiv:1012.1792](#) [hep-ex]
37. A. Martin, W. Stirling, R. Thorne, G. Watt, Parton distributions for the LHC. *Eur. Phys. J. C Part. Fields* **63**, 189–285 (2009). [arXiv:0901.0002](#) [hep-ph]
38. C.-H. Kom, W. Stirling, Charge asymmetry in $W +$ jets production at the LHC. *Eur. Phys. J. C Part. Fields* **69**, 67–73 (2010). [arXiv:1004.3404](#) [hep-ph]
39. G. D’Agostini, A multidimensional unfolding method based on Bayes’ theorem. *Nucl. Instrum. Methods A* **362**, 487–498 (1995)
40. ATLAS Collaboration, Jet energy resolution and selection efficiency relative to track jets from in-situ techniques with the ATLAS detector using proton–proton collisions at a center of mass energy $\sqrt{s} = 7$ TeV. ATLAS-CONF-2010-054 (2010). <http://cdsweb.cern.ch/record/1281311>
41. ATLAS Collaboration, Luminosity determination in pp collisions at $\sqrt{s} = 7$ TeV using the ATLAS detector at the LHC. *Eur. Phys. J. C* **71**, 1630 (2011). [arXiv:1101.2185](#) [hep-ex]
42. ATLAS Collaboration, Updated luminosity determination in pp collisions at $\sqrt{s} = 7$ TeV using the ATLAS detector. ATLAS-CONF-2011-011 (2011). <http://cdsweb.cern.ch/record/1334563/>
43. P. Nason, A new method for combining NLO QCD with shower Monte Carlo algorithms. *J. High Energy Phys.* **11**, 040 (2004). [arXiv:hep-ph/0409146](#)
44. S. Frixione, P. Nason, C. Oleari, Matching NLO QCD computations with Parton Shower simulations: the POWHEG method. *J. High Energy Phys.* **11**, 070 (2007). [arXiv:0709.2092](#) [hep-ph]
45. B.P. Kersevan, E. Richter-Was, The Monte Carlo event generator AcerMC version 3.5 with interfaces to PYTHIA 6.4, HERWIG 6.5 and ARIADNE 4.1. [hep-ph/0405247](#)
46. ATLAS Collaboration, Expected performance of the ATLAS experiment—detector, trigger and physics, pp. 870–883 (2009). [arXiv:0901.0512](#) [hep-ex]
47. P.Z. Skands, Tuning Monte Carlo generators: the Perugia tunes. *Phys. Rev. D* **82**, 074018 (2010). [arXiv:1005.3457](#) [hep-ph]
48. M. Botje et al., The PDF4LHC working group interim recommendations. [arXiv:1101.0538](#) [hep-ph]
49. Tevatron Electroweak Working Group Collaboration, Combination of CDF and D0 results on the mass of the top quark using up to 5.8 fb^{-1} of data (2011). [arXiv:1107.5255](#) [hep-ex]
50. F.A. Berends, H. Kuijf, B. Tausk, W.T. Giele, On the production of a W and jets at hadron colliders. *Nucl. Phys. B* **357**, 32–64 (1991)
51. T. Gleisberg et al., Event generation with SHERPA 1.1. *J. High Energy Phys.* **02**, 007 (2009). [arXiv:0811.4622](#) [hep-ph]
52. L. Lyons, D. Gibaut, P. Clifford, How to combine correlated estimates of a single physical quantity. *Nucl. Instrum. Methods A* **270**, 110 (1988)
53. A. Valassi, Combining correlated measurements of several different physical quantities. *Nucl. Instrum. Methods A* **500**, 391–405 (2003)
54. J.H. Kühn, G. Rodrigo, Charge asymmetries of top quarks at hadron colliders revisited. *J. High Energy Phys.* **1201**, 063 (2012). [arXiv:1109.6830](#) [hep-ph]
55. J. Aguilar-Saavedra, M. Perez-Victoria, Simple models for the top asymmetry: constraints and predictions. *J. High Energy Phys.* **1109**, 097 (2011). [arXiv:1107.0841](#) [hep-ph]
56. J. Aguilar-Saavedra, Single top quark production at LHC with anomalous Wtb couplings. *Nucl. Phys. B* **804**, 160–192 (2008). [arXiv:0803.3810](#) [hep-ph]
57. ATLAS Collaboration, Search for same-sign top-quark production and fourth-generation down-type quarks in pp collisions at $\sqrt{s} = 7\text{TeV}$ with the ATLAS detector. *J. High Energy Phys.* **1204**, 069 (2012). [arXiv:1202.5520](#) [hep-ex]
58. W. Hollik, D. Pagani, The electroweak contribution to the top quark forward–backward asymmetry at the Tevatron. *Phys. Rev. D* **84**, 093003 (2011). [arXiv:1107.2606](#) [hep-ph]
59. V. Ahrens, A. Ferroglia, M. Neubert, B.D. Pecjak, L.L. Yang, The top-pair forward–backward asymmetry beyond NLO. *Phys. Rev. D* **84**, 074004 (2011). [arXiv:1106.6051](#) [hep-ph]

The ATLAS Collaboration

G. Aad⁴⁸, B. Abbott¹¹⁰, J. Abdallah¹¹, A.A. Abdelalim⁴⁹, A. Abdesselam¹¹⁷, O. Abidinov¹⁰, B. Abi¹¹¹, M. Abolins⁸⁷, O.S. AbouZeid¹⁵⁷, H. Abramowicz¹⁵², H. Abreu¹¹⁴, E. Acerbi^{88a,88b}, B.S. Acharya^{163a,163b}, L. Adamczyk³⁷, D.L. Adams²⁴,

T.N. Addy⁵⁶, J. Adelman¹⁷⁴, M. Aderholz⁹⁸, S. Adomeit⁹⁷, P. Adragna⁷⁴, T. Adye¹²⁸, S. Aefsky²², J.A. Aguilar-Saavedra^{123b,a}, M. Aharrouche⁸⁰, S.P. Ahlen²¹, F. Ahles⁴⁸, A. Ahmad¹⁴⁷, M. Ahsan⁴⁰, G. Aielli^{132a,132b}, T. Akdogan^{18a}, T.P.A. Åkesson⁷⁸, G. Akimoto¹⁵⁴, A.V. Akimov⁹³, A. Akiyama⁶⁶, M.S. Alam¹, M.A. Alam⁷⁵, J. Albert¹⁶⁸, S. Albrand⁵⁵, M. Aleksa²⁹, I.N. Aleksandrov⁶⁴, F. Alessandria^{88a}, C. Alexa^{25a}, G. Alexander¹⁵², G. Alexandre⁴⁹, T. Alexopoulos⁹, M. Alhroob²⁰, M. Aliev¹⁵, G. Alimonti^{88a}, J. Alison¹¹⁹, M. Aliyev¹⁰, P.P. Allport⁷², S.E. Allwood-Spiers⁵³, J. Almond⁸¹, A. Aloisio^{101a,101b}, R. Alon¹⁷⁰, A. Alonso⁷⁸, B. Alvarez Gonzalez⁸⁷, M.G. Alviggi^{101a,101b}, K. Amako⁶⁵, P. Amaral²⁹, C. Amelung²², V.V. Ammosov¹²⁷, A. Amorim^{123a,b}, G. Amorós¹⁶⁶, N. Amram¹⁵², C. Anastopoulos²⁹, L.S. Ancu¹⁶, N. Andari¹¹⁴, T. Andeen³⁴, C.F. Anders²⁰, G. Anders^{58a}, K.J. Anderson³⁰, A. Andreazza^{88a,88b}, V. Andrei^{58a}, M-L. Andrieux⁵⁵, X.S. Anduaga⁶⁹, A. Angerami³⁴, F. Anghinolfi²⁹, A. Anisenkov¹⁰⁶, N. Anjos^{123a}, A. Annovi⁴⁷, A. Antonaki⁸, M. Antonelli⁴⁷, A. Antonov⁹⁵, J. Antos^{143b}, F. Anulli^{131a}, S. Aoun⁸², L. Aperio Bella⁴, R. Apolle^{117,c}, G. Arabidze⁸⁷, I. Aracena¹⁴², Y. Arai⁶⁵, A.T.H. Arce⁴⁴, J.P. Archambault²⁸, S. Arfaoui¹⁴⁷, J-F. Arguin¹⁴, E. Arik^{18a,*}, M. Arik^{18a}, A.J. Armbruster⁸⁶, O. Arnaez⁸⁰, C. Arnault¹¹⁴, A. Artamonov⁹⁴, G. Artoni^{131a,131b}, D. Arutinov²⁰, S. Asai¹⁵⁴, R. Asfandiyarov¹⁷¹, S. Ask²⁷, B. Åsman^{145a,145b}, L. Asquith⁵, K. Assamagan²⁴, A. Astbury¹⁶⁸, A. Astvatsatourov⁵², B. Aubert⁴, E. Auge¹¹⁴, K. Augsten¹²⁶, M. Aurousseau^{144a}, G. Avolio¹⁶², R. Avramidou⁹, D. Axen¹⁶⁷, C. Ay⁵⁴, G. Azuelos^{92,d}, Y. Azuma¹⁵⁴, M.A. Baak²⁹, G. Baccaglioni^{88a}, C. Bacci^{133a,133b}, A.M. Bach¹⁴, H. Bachacou¹³⁵, K. Bachas²⁹, G. Bachy²⁹, M. Backes⁴⁹, M. Backhaus²⁰, E. Badescu^{25a}, P. Bagnaia^{131a,131b}, S. Bahinipati², Y. Bai^{32a}, D.C. Bailey¹⁵⁷, T. Bain¹⁵⁷, J.T. Baines¹²⁸, O.K. Baker¹⁷⁴, M.D. Baker²⁴, S. Baker⁷⁶, E. Banas³⁸, P. Banerjee⁹², Sw. Banerjee¹⁷¹, D. Banfi²⁹, A. Bangert¹⁴⁹, V. Bansal¹⁶⁸, H.S. Bansil¹⁷, L. Barak¹⁷⁰, S.P. Baranov⁹³, A. Barashkou⁶⁴, A. Barbaro Galtieri¹⁴, T. Barber⁴⁸, E.L. Barberio⁸⁵, D. Barberis^{50a,50b}, M. Barbero²⁰, D.Y. Bardin⁶⁴, T. Barillari⁹⁸, M. Barisonzi¹⁷³, T. Barklow¹⁴², N. Barlow²⁷, B.M. Barnett¹²⁸, R.M. Barnett¹⁴, A. Baroncelli^{133a}, G. Barone⁴⁹, A.J. Barr¹¹⁷, F. Barreiro⁷⁹, J. Barreiro Guimarães da Costa⁵⁷, P. Barrillon¹¹⁴, R. Bartoldus¹⁴², A.E. Barton⁷⁰, V. Bartsch¹⁴⁸, R.L. Bates⁵³, L. Batkova^{143a}, J.R. Batley²⁷, A. Battaglia¹⁶, M. Battistin²⁹, F. Bauer¹³⁵, H.S. Bawa^{142,e}, S. Beale⁹⁷, B. Beare¹⁵⁷, T. Beau⁷⁷, P.H. Beauchemin¹⁶⁰, R. Beccherle^{50a}, P. Bechtel²⁰, H.P. Beck¹⁶, S. Becker⁹⁷, M. Beckingham¹³⁷, K.H. Becks¹⁷³, A.J. Beddall^{18c}, A. Beddall^{18c}, S. Bedikian¹⁷⁴, V.A. Bednyakov⁶⁴, C.P. Bee⁸², M. Begel²⁴, S. Behar Harpaz¹⁵¹, P.K. Behara⁶², M. Beimforde⁹⁸, C. Belanger-Champagne⁸⁴, P.J. Bell⁴⁹, W.H. Bell⁴⁹, G. Bella¹⁵², L. Bellagamba^{19a}, F. Bellina²⁹, M. Bellomo²⁹, A. Belloni⁵⁷, O. Beloborodova^{106,f}, K. Belotskiy⁹⁵, O. Beltramello²⁹, S. Ben Ami¹⁵¹, O. Benary¹⁵², D. Benchechroun^{134a}, C. Benchouk⁸², M. Bendel⁸⁰, N. Benekos¹⁶⁴, Y. Benhammou¹⁵², E. Benhar Nocchioli⁴⁹, J.A. Benitez Garcia^{158b}, D.P. Benjamin⁴⁴, M. Benoit¹¹⁴, J.R. Bensinger²², K. Benslama¹²⁹, S. Bentvelsen¹⁰⁴, D. Berge²⁹, E. Bergeaas Kuutmann⁴¹, N. Berger⁴, F. Berghaus¹⁶⁸, E. Berglund¹⁰⁴, J. Beringer¹⁴, P. Bernat⁷⁶, R. Bernhard¹⁴⁸, C. Bernius²⁴, T. Berry⁷⁵, C. Bertella⁸², A. Bertin^{19a,19b}, F. Bertinelli²⁹, F. Bertolucci^{121a,121b}, M.I. Besana^{88a,88b}, N. Besson¹³⁵, S. Bethke⁹⁸, W. Bhimji⁴⁵, R.M. Bianchi²⁹, M. Bianco^{71a,71b}, O. Biebel⁹⁷, S.P. Bieniek⁷⁶, K. Bierwagen⁵⁴, J. Biesiada¹⁴, M. Biglietti^{133a}, H. Bilokon⁴⁷, M. Bindi^{19a,19b}, S. Binet¹¹⁴, A. Bingul^{18c}, C. Bini^{131a,131b}, C. Biscarat¹⁷⁶, U. Bitenc⁴⁸, K.M. Black²¹, R.E. Blair⁵, J.-B. Blanchard¹³⁵, G. Blanchot²⁹, T. Blazek^{143a}, C. Blocker²², J. Blocki³⁸, A. Blondel⁴⁹, W. Blum⁸⁰, U. Blumenschein⁵⁴, G.J. Bobbink¹⁰⁴, V.B. Bobrovnikov¹⁰⁶, S.S. Bocchetta⁷⁸, A. Bocci⁴⁴, C.R. Boddy¹¹⁷, M. Boehler⁴¹, J. Boek¹⁷³, N. Boelaert³⁵, S. Böser⁷⁶, J.A. Bogaerts²⁹, A. Bogdanchikov¹⁰⁶, A. Bogouch^{89,*}, C. Bohm^{145a}, V. Boisvert⁷⁵, T. Bold³⁷, V. Boldea^{25a}, N.M. Bolnet¹³⁵, M. Bona⁷⁴, V.G. Bondarenko⁹⁵, M. Bondioli¹⁶², M. Boonekamp¹³⁵, G. Boorman⁷⁵, C.N. Booth¹³⁸, S. Bordini⁷⁷, C. Borer¹⁶, A. Borisov¹²⁷, G. Borissov⁷⁰, I. Borjanovic^{12a}, M. Borri⁸¹, S. Borroni⁸⁶, K. Bos¹⁰⁴, D. Boscherini^{19a}, M. Bosman¹¹, H. Boterenbrood¹⁰⁴, D. Botterill¹²⁸, J. Bouchami⁹², J. Boudreau¹²², E.V. Bouhova-Thacker⁷⁰, D. Boumediene³³, C. Bourdarios¹¹⁴, N. Bousson⁸², A. Boveia³⁰, J. Boyd²⁹, I.R. Boyko⁶⁴, N.I. Bozhko¹²⁷, I. Bozovic-Jelisavcic^{12b}, J. Bracinik¹⁷, A. Braem²⁹, P. Branchini^{133a}, G.W. Brandenburg⁵⁷, A. Brandt⁷, G. Brandt¹¹⁷, O. Brandt⁵⁴, U. Bratzler¹⁵⁵, B. Brau⁸³, J.E. Brau¹¹³, H.M. Braun¹⁷³, B. Brelief¹⁵⁷, J. Bremer²⁹, R. Brenner¹⁶⁵, S. Bressler¹⁷⁰, D. Breton¹¹⁴, D. Britton⁵³, F.M. Brochu²⁷, I. Brock²⁰, R. Brock⁸⁷, T.J. Brodbeck⁷⁰, E. Brodet¹⁵², F. Broggi^{88a}, C. Bromberg⁸⁷, J. Bronner⁹⁸, G. Brooijmans³⁴, W.K. Brooks^{31b}, G. Brown⁸¹, H. Brown⁷, P.A. Bruckman de Renstrom³⁸, D. Bruncko^{143b}, R. Bruneliere⁴⁸, S. Brunet⁶⁰, A. Bruni^{19a}, G. Bruni^{19a}, M. Bruschi^{19a}, T. Buanes¹³, Q. Buat⁵⁵, F. Bucci⁴⁹, J. Buchanan¹¹⁷, N.J. Buchanan², P. Buchholz¹⁴⁰, R.M. Buckingham¹¹⁷, A.G. Buckley⁴⁵, S.I. Buda^{25a}, I.A. Budagov⁶⁴, B. Budick¹⁰⁷, V. Büscher⁸⁰, L. Bugge¹¹⁶, O. Bulekov⁹⁵, M. Bunse⁴², T. Buran¹¹⁶, H. Burckhart²⁹, S. Burdin⁷², T. Burgess¹³, S. Burke¹²⁸, E. Busato³³, P. Bussey⁵³, C.P. Buszello¹⁶⁵, F. Butin²⁹, B. Butler¹⁴², J.M. Butler²¹, C.M. Buttar⁵³, J.M. Butterworth⁷⁶, W. Buttinger²⁷, S. Cabrera Urbán¹⁶⁶, D. Caforio^{19a,19b}, O. Cakir^{3a}, P. Calafiura¹⁴, G. Calderini⁷⁷, P. Calfayan⁹⁷, R. Calkins¹⁰⁵, L.P. Caloba^{23a}, R. Caloi^{131a,131b}, D. Calvet³³, S. Calvet³³, R. Camacho Toro³³, P. Camarri^{132a,132b}, M. Cambiaghi^{118a,118b}, D. Cameron¹¹⁶, L.M. Caminada¹⁴, S. Campana²⁹, M. Campanelli⁷⁶, V. Canale^{101a,101b}, F. Canelli^{30,g}, A. Canepa^{158a}, J. Cantero⁷⁹, L. Capasso^{101a,101b}, M.D.M. Capeans Garrido²⁹, I. Caprini^{25a}, M. Caprini^{25a}, D. Capriotti⁹⁸, M. Capua^{36a,36b}, R. Caputo⁸⁰, C. Caramarcu²⁴, R. Cardarelli^{132a}, T. Carli²⁹, G. Carlino^{101a}, L. Carminati^{88a,88b}, B. Caron⁸⁴, S. Caron¹⁰³, G.D. Carrillo Montoya¹⁷¹, A.A. Carter⁷⁴, J.R. Carter²⁷,

J. Carvalho^{123a,h}, D. Casadei¹⁰⁷, M.P. Casado¹¹, M. Cascella^{121a,121b}, C. Caso^{50a,50b,*}, A.M. Castaneda Hernandez¹⁷¹, E. Castaneda-Miranda¹⁷¹, V. Castillo Gimenez¹⁶⁶, N.F. Castro^{123a}, G. Cataldi^{71a}, F. Cataneo²⁹, A. Catinaccio²⁹, J.R. Catmore²⁹, A. Cattai²⁹, G. Cattani^{132a,132b}, S. Caughron⁸⁷, D. Cauz^{163a,163c}, P. Cavalleri⁷⁷, D. Cavalli^{88a}, M. Cavalli-Sforza¹¹, V. Cavasinni^{121a,121b}, F. Ceradini^{133a,133b}, A.S. Cerqueira^{23b}, A. Cerri²⁹, L. Cerrito⁷⁴, F. Cerutti⁴⁷, S.A. Cetin⁸⁶, F. Cevenini^{101a,101b}, A. Chafaq^{134a}, D. Chakraborty¹⁰⁵, K. Chan², B. Chapleau⁸⁴, J.D. Chapman²⁷, J.W. Chapman⁸⁶, E. Chareyre⁷⁷, D.G. Charlton¹⁷, V. Chavda⁸¹, C.A. Chavez Barajas²⁹, S. Cheatham⁸⁴, S. Chekanov⁵, S.V. Chekulaev^{158a}, G.A. Chelkov⁶⁴, M.A. Chelstowska¹⁰³, C. Chen⁶³, H. Chen²⁴, S. Chen^{32c}, T. Chen^{32c}, X. Chen¹⁷¹, S. Cheng^{32a}, A. Cheplakov⁶⁴, V.F. Chepurnov⁶⁴, R. Cherkaoui El Moursli^{134e}, V. Chernyatin²⁴, E. Cheu⁶, S.L. Cheung¹⁵⁷, L. Chevalier¹³⁵, G. Chiefari^{101a,101b}, L. Chikovani^{51a}, J.T. Childers²⁹, A. Chilingarov⁷⁰, G. Chiodini^{71a}, M.V. Chizhov⁶⁴, G. Choudalakis³⁰, S. Chouridou¹³⁶, I.A. Christidi⁷⁶, A. Christov⁴⁸, D. Chromek-Burckhart²⁹, M.L. Chu¹⁵⁰, J. Chudoba¹²⁴, G. Ciapetti^{131a,131b}, K. Ciba³⁷, A.K. Ciftci^{3a}, R. Ciftci^{3a}, D. Cinca³³, V. Cindro⁷³, M.D. Ciobotaru¹⁶², C. Ciocca^{19a}, A. Ciochio¹⁴, M. Cirilli⁸⁶, M. Citterio^{88a}, M. Ciubancan^{25a}, A. Clark⁴⁹, P.J. Clark⁴⁵, W. Cleland¹²², J.C. Clemens⁸², B. Clement⁵⁵, C. Clement^{145a,145b}, R.W. Clifft¹²⁸, Y. Coadou⁸², M. Cobal^{163a,163c}, A. Coccaro¹⁷¹, J. Cochran⁶³, P. Coe¹¹⁷, J.G. Cogan¹⁴², J. Coggeshall¹⁶⁴, E. Cogneras¹⁷⁶, J. Colas⁴, A.P. Colijn¹⁰⁴, N.J. Collins¹⁷, C. Collins-Tooth⁵³, J. Collot⁵⁵, G. Colon⁸³, P. Conde Muñio^{123a}, E. Coniavitis¹¹⁷, M.C. Conidi¹¹, M. Consonni¹⁰³, V. Consorti⁴⁸, S. Constantinescu^{25a}, C. Conta^{118a,118b}, F. Conventi^{101a,i}, J. Cook²⁹, M. Cooke¹⁴, B.D. Cooper⁷⁶, A.M. Cooper-Sarkar¹¹⁷, K. Copic¹⁴, T. Cornelissen¹⁷³, M. Corradi^{19a}, F. Corriveau^{84,j}, A. Cortes-Gonzalez¹⁶⁴, G. Cortiana⁹⁸, G. Costa^{88a}, M.J. Costa¹⁶⁶, D. Costanzo¹³⁸, T. Costin³⁰, D. Côte²⁹, R. Coura Torres^{23a}, L. Courneyea¹⁶⁸, G. Cowan⁷⁵, C. Cowden²⁷, B.E. Cox⁸¹, K. Cranmer¹⁰⁷, F. Crescioli^{121a,121b}, M. Cristinziani²⁰, G. Crosetti^{36a,36b}, R. Crupi^{71a,71b}, S. Crépe-Renaudin⁵⁵, C.-M. Cuciuc^{25a}, C. Cuenca Almenar¹⁷⁴, T. Cuhadar Donszelmann¹³⁸, M. Curatolo⁴⁷, C.J. Curtis¹⁷, C. Cuthbert¹⁴⁹, P. Cwetanski⁶⁰, H. Czirr¹⁴⁰, P. Czodrowski⁴³, Z. Czyczula¹⁷⁴, S. D'Auria⁵³, M. D'Onofrio⁷², A. D'Orazio^{131a,131b}, P.V.M. Da Silva^{23a}, C. Da Via⁸¹, W. Dabrowski³⁷, T. Dai⁸⁶, C. Dallapiccola⁸³, M. Dam³⁵, M. Dameri^{50a,50b}, D.S. Damiani¹³⁶, H.O. Danielsson²⁹, D. Dannheim⁹⁸, V. Dao⁴⁹, G. Darbo^{50a}, G.L. Darlea^{25b}, C. Daum¹⁰⁴, W. Davey²⁰, T. Davidek¹²⁵, N. Davidson⁸⁵, R. Davidson⁷⁰, E. Davies^{117,c}, M. Davies⁹², A.R. Davison⁷⁶, Y. Davygora^{58a}, E. Dawe¹⁴¹, I. Dawson¹³⁸, J.W. Dawson^{5,*}, R.K. Daya-Ishmukhametova²², K. De⁷, R. de Asmundis^{101a}, S. De Castro^{19a,19b}, P.E. De Castro Faria Salgado²⁴, S. De Cecco⁷⁷, J. de Graat⁹⁷, N. De Groot¹⁰³, P. de Jong¹⁰⁴, C. De La Taille¹¹⁴, H. De la Torre⁷⁹, B. De Lotto^{163a,163c}, L. de Mora⁷⁰, L. De Nooij¹⁰⁴, D. De Pedis^{131a}, A. De Salvo^{131a}, U. De Sanctis^{163a,163c}, A. De Santo¹⁴⁸, J.B. De Vivie De Regie¹¹⁴, S. Dean⁷⁶, W.J. Dearnaley⁷⁰, R. Debbe²⁴, C. Debenedetti⁴⁵, D.V. Dedovich⁶⁴, J. Degenhardt¹¹⁹, M. Dehchar¹¹⁷, C. Del Papa^{163a,163c}, J. Del Peso⁷⁹, T. Del Prete^{121a,121b}, T. Delemontex⁵⁵, M. Deliyergiyev⁷³, A. Dell'Acqua²⁹, L. Dell'Asta²¹, M. Della Pietra^{101a,i}, D. della Volpe^{101a,101b}, M. Delmastro⁴, N. Delruelle²⁹, P.A. Delsart⁵⁵, C. Deluca¹⁴⁷, S. Demers¹⁷⁴, M. Demichev⁶⁴, B. Demirkoz^{11,k}, J. Deng¹⁶², S.P. Denisov¹²⁷, D. Derendarz³⁸, J.E. Derkaoui^{134d}, F. Derue⁷⁷, P. Dervan⁷², K. Desch²⁰, E. Devetak¹⁴⁷, P.O. Deviveiros¹⁰⁴, A. Dewhurst¹²⁸, B. DeWilde¹⁴⁷, S. Dhaliwal¹⁵⁷, R. Dhullipudi^{24,1}, A. Di Ciaccio^{132a,132b}, L. Di Ciaccio⁴, A. Di Girolamo²⁹, B. Di Girolamo²⁹, S. Di Luise^{133a,133b}, A. Di Mattia¹⁷¹, B. Di Micco²⁹, R. Di Nardo⁴⁷, A. Di Simone^{132a,132b}, R. Di Sipio^{19a,19b}, M.A. Diaz^{31a}, F. Diblen^{18c}, E.B. Diehl⁸⁶, J. Dietrich⁴¹, T.A. Dietzsch^{58a}, S. Diglio⁸⁵, K. Dindar Yagci³⁹, J. Dingfelder²⁰, C. Dionisi^{131a,131b}, P. Dita^{25a}, S. Dita^{25a}, F. Dittus²⁹, F. Djama⁸², T. Djobava^{51b}, M.A.B. do Vale^{23c}, A. Do Valle Wemans^{123a}, T.K.O. Doan⁴, M. Dobbs⁸⁴, R. Dobinson^{29,*}, D. Dobos²⁹, E. Dobson^{29,m}, J. Dodd³⁴, C. Doglioni⁴⁹, T. Doherty⁵³, Y. Doi^{65,*}, J. Dolejsi¹²⁵, I. Dolenc⁷³, Z. Dolezal¹²⁵, B.A. Dolgoshein^{95,*}, T. Dohmae¹⁵⁴, M. Donadelli^{23d}, M. Donega¹¹⁹, J. Donini³³, J. Dopke²⁹, A. Doria^{101a}, A. Dos Anjos¹⁷¹, M. Dosit¹¹, A. Dotti^{121a,121b}, M.T. Dova⁶⁹, J.D. Dowell¹⁷, A.D. Doxiadis¹⁰⁴, A.T. Doyle⁵³, Z. Drasal¹²⁵, J. Drees¹⁷³, N. Dressnandt¹¹⁹, H. Drevermann²⁹, C. Driouichi³⁵, M. Dris⁹, J. Dubbert⁹⁸, S. Dube¹⁴, E. Duchovni¹⁷⁰, G. Duckeck⁹⁷, A. Dudarev²⁹, F. Dudziak⁶³, M. Dührssen²⁹, I.P. Duerdoth⁸¹, L. Dufloc¹¹⁴, M.-A. Dufour⁸⁴, M. Dunford²⁹, H. Duran Yildiz^{3a}, R. Duxfield¹³⁸, M. Dwuznik³⁷, F. Dydak²⁹, M. Düren⁵², W.L. Ebenstein⁴⁴, J. Ebke⁹⁷, S. Eckweiler⁸⁰, K. Edmonds⁸⁰, C.A. Edwards⁷⁵, N.C. Edwards⁵³, W. Ehrenfeld⁴¹, T. Ehrich⁹⁸, T. Eifert¹⁴², G. Eigen¹³, K. Einsweiler¹⁴, E. Eisenhandler⁷⁴, T. Ekelof¹⁶⁵, M. El Kacimi^{134c}, M. Ellert¹⁶⁵, S. Elles⁴, F. Ellinghaus⁸⁰, K. Ellis⁷⁴, N. Ellis²⁹, J. Elmsheuser⁹⁷, M. Elsing²⁹, D. Emel'yanov¹²⁸, R. Engelmann¹⁴⁷, A. Engl⁹⁷, B. Epp⁶¹, A. Eppig⁸⁶, J. Erdmann⁵⁴, A. Ereditato¹⁶, D. Eriksson^{145a}, J. Ernst¹, M. Ernst²⁴, J. Ernwein¹³⁵, D. Errede¹⁶⁴, S. Errede¹⁶⁴, E. Ertel⁸⁰, M. Escalier¹¹⁴, C. Escobar¹²², X. Espinal Curull¹¹, B. Esposito⁴⁷, F. Etienne⁸², A.I. Etievre¹³⁵, E. Etzion¹⁵², D. Evangelakou⁵⁴, H. Evans⁶⁰, L. Fabbri^{19a,19b}, C. Fabre²⁹, R.M. Fakhruddinov¹²⁷, S. Falciano^{131a}, Y. Fang¹⁷¹, M. Fanti^{88a,88b}, A. Farbin⁷, A. Farilla^{133a}, J. Farley¹⁴⁷, T. Faro Roque¹⁵⁷, S.M. Farrington¹¹⁷, P. Farthouat²⁹, P. Fassnacht²⁹, D. Fassouliotis⁸, B. Fatholahzadeh¹⁵⁷, A. Favareto^{88a,88b}, L. Fayard¹¹⁴, S. Fazio^{36a,36b}, R. Febbraro³³, P. Federic^{143a}, O.L. Fedin¹²⁰, W. Fedorko⁸⁷, M. Fehling-Kaschek⁴⁸, L. Felgion⁸², D. Fellmann⁵, C. Feng^{32d}, E.J. Feng³⁰, A.B. Fenyuk¹²⁷, J. Ferencei^{143b}, J. Ferland⁹², W. Fernando¹⁰⁸, S. Ferrag⁵³, J. Ferrando⁵³, V. Ferrara⁴¹, A. Ferrari¹⁶⁵, P. Ferrari¹⁰⁴, R. Ferrari^{118a}, A. Ferrer¹⁶⁶, M.L. Ferrer⁴⁷, D. Ferrere⁴⁹, C. Ferretti⁸⁶, A. Ferretto Parodi^{50a,50b}, M. Fiascaris³⁰, F. Fiedler⁸⁰, A. Filipčič⁷³, A. Philippas⁹, F. Filthaut¹⁰³, M. Fincke-Keeler¹⁶⁸, M.C.N. Fiolhais^{123a,h}, L. Fiorini¹⁶⁶, A. Firan³⁹, G. Fischer⁴¹, P. Fischer²⁰, M.J. Fisher¹⁰⁸, M. Flechl⁴⁸, I. Fleck¹⁴⁰

J. Fleckner⁸⁰, P. Fleischmann¹⁷², S. Fleischmann¹⁷³, T. Flick¹⁷³, L.R. Flores Castillo¹⁷¹, M.J. Flowerdew⁹⁸, M. Fokitis⁹, T. Fonseca Martin¹⁶, D.A. Forbush¹³⁷, A. Formica¹³⁵, A. Forti⁸¹, D. Fortin^{158a}, J.M. Foster⁸¹, D. Fournier¹¹⁴, A. Foussat²⁹, A.J. Fowler⁴⁴, K. Fowler¹³⁶, H. Fox⁷⁰, P. Francavilla¹¹, S. Franchino^{118a,118b}, D. Francis²⁹, T. Frank¹⁷⁰, M. Franklin⁵⁷, S. Franz²⁹, M. Fraternali^{118a,118b}, S. Fratina¹¹⁹, S.T. French²⁷, F. Friedrich⁴³, R. Froeschl²⁹, D. Froidevaux²⁹, J.A. Frost²⁷, C. Fukunaga¹⁵⁵, E. Fullana Torregrosa²⁹, J. Fuster¹⁶⁶, C. Gabaldon²⁹, O. Gabizon¹⁷⁰, T. Gadfort²⁴, S. Gadomski⁴⁹, G. Gagliardi^{50a,50b}, P. Gagnon⁶⁰, C. Galea⁹⁷, E.J. Gallas¹¹⁷, V. Gallo¹⁶, B.J. Gallop¹²⁸, P. Gallus¹²⁴, K.K. Gan¹⁰⁸, Y.S. Gao^{142e}, V.A. Gapienko¹²⁷, A. Gaponenko¹⁴, F. Garberson¹⁷⁴, M. Garcia-Sciveres¹⁴, C. García¹⁶⁶, J.E. García Navarro¹⁶⁶, R.W. Gardner³⁰, N. Garelli²⁹, H. Garitaonandia¹⁰⁴, V. Garonne²⁹, J. Garvey¹⁷, C. Gatti⁴⁷, G. Gaudio^{118a}, O. Gaumer⁴⁹, B. Gaur¹⁴⁰, L. Gauthier¹³⁵, I.L. Gavrilenko⁹³, C. Gay¹⁶⁷, G. Gaycken²⁰, J.-C. Gayde²⁹, E.N. Gazis⁹, P. Ge^{32d}, C.N.P. Gee¹²⁸, D.A.A. Geerts¹⁰⁴, Ch. Geich-Gimbel²⁰, K. Gellerstedt^{145a,145b}, C. Gemme^{50a}, A. Gemmell⁵³, M.H. Genest⁵⁵, S. Gentile^{131a,131b}, M. George⁵⁴, S. George⁷⁵, P. Gerlach¹⁷³, A. Gershon¹⁵², C. Geweniger^{58a}, H. Ghazlane^{134b}, N. Ghodbane³³, B. Giacobbe^{19a}, S. Giagu^{131a,131b}, V. Giakoumopoulou⁸, V. Giangiobbe¹¹, F. Gianotti²⁹, B. Gibbard²⁴, A. Gibson¹⁵⁷, S.M. Gibson²⁹, L.M. Gilbert¹¹⁷, V. Gilevsky⁹⁰, D. Gillberg²⁸, A.R. Gillman¹²⁸, D.M. Gingrich^{2,d}, J. Ginzburg¹⁵², N. Giokaris⁸, M.P. Giordani^{163c}, R. Giordano^{101a,101b}, F.M. Giorgi¹⁵, P. Giovannini⁹⁸, P.F. Giraud¹³⁵, D. Giugni^{88a}, M. Giunta⁹², P. Giusti^{19a}, B.K. Gjelsten¹¹⁶, L.K. Gladilin⁹⁶, C. Glasman⁷⁹, J. Glatzer⁴⁸, A. Glazov⁴¹, K.W. Glitza¹⁷³, G.L. Glonti⁶⁴, J.R. Goddard⁷⁴, J. Godfrey¹⁴¹, J. Godlewski²⁹, M. Goebel⁴¹, T. Göpfert⁴³, C. Goeringer⁸⁰, C. Gössling⁴², T. Göttfert⁹⁸, S. Goldfarb⁸⁶, T. Golling¹⁷⁴, S.N. Golovnia¹²⁷, A. Gomes^{123a,b}, L.S. Gomez Fajardo⁴¹, R. Gonçalo⁷⁵, J. Goncalves Pinto Firmino Da Costa⁴¹, L. Gonella²⁰, A. Gonidec²⁹, S. Gonzalez¹⁷¹, S. González de la Hoz¹⁶⁶, G. Gonzalez Parra¹¹, M.L. Gonzalez Silva²⁶, S. Gonzalez-Sevilla⁴⁹, J.J. Goodson¹⁴⁷, L. Goossens²⁹, P.A. Gorbounov⁹⁴, H.A. Gordon²⁴, I. Gorelov¹⁰², G. Gorfine¹⁷³, B. Gorini²⁹, E. Gorini^{71a,71b}, A. Gorišek⁷³, E. Gornicki³⁸, S.A. Gorokhov¹²⁷, V.N. Goryachev¹²⁷, B. Gosdzik⁴¹, M. Gosselink¹⁰⁴, M.I. Gostkin⁶⁴, I. Gough Eschrich¹⁶², M. Gouighri^{134a}, D. Goujdami^{134c}, M.P. Goulette⁴⁹, A.G. Goussiou¹³⁷, C. Goy⁴, S. Gozpinar²², I. Grabowska-Bold³⁷, P. Grafström²⁹, K.-J. Grahm⁴¹, F. Grancagnolo^{71a}, S. Grancagnolo¹⁵, V. Grassi¹⁴⁷, V. Gratchev¹²⁰, N. Grau³⁴, H.M. Gray²⁹, J.A. Gray¹⁴⁷, E. Graziani^{133a}, O.G. Grebenyuk¹²⁰, T. Greenshaw⁷², Z.D. Greenwood^{24,1}, K. Gregersen³⁵, I.M. Gregor⁴¹, P. Grenier¹⁴², J. Griffiths¹³⁷, N. Grigalashvili⁶⁴, A.A. Grillo¹³⁶, S. Grinstein¹¹, Y.V. Grishkevich⁹⁶, J.-F. Grivaz¹¹⁴, M. Groh⁹⁸, E. Gross¹⁷⁰, J. Grosse-Knetter⁵⁴, J. Groth-Jensen¹⁷⁰, K. Grybel¹⁴⁰, V.J. Guarino⁵, D. Guest¹⁷⁴, C. Guicheney³³, A. Guida^{71a,71b}, S. Guindon⁵⁴, H. Guler^{84,n}, J. Gunther¹²⁴, B. Guo¹⁵⁷, J. Guo³⁴, A. Gupta³⁰, Y. Gusakov⁶⁴, V.N. Gushchin¹²⁷, A. Gutierrez⁹², P. Gutierrez¹¹⁰, N. Guttman¹⁵², O. Gutzwiller¹⁷¹, C. Guyot¹³⁵, C. Gwenlan¹¹⁷, C.B. Gwilliam⁷², A. Haas¹⁴², S. Haas²⁹, C. Haber¹⁴, H.K. Hadavand³⁹, D.R. Hadley¹⁷, P. Haefner⁹⁸, F. Hahn²⁹, S. Haider²⁹, Z. Hajduk³⁸, H. Hakobyan¹⁷⁵, D. Hall¹¹⁷, J. Haller⁵⁴, K. Hamacher¹⁷³, P. Hamal¹¹², M. Hamer⁵⁴, A. Hamilton^{144b,o}, S. Hamilton¹⁶⁰, H. Han^{32a}, L. Han^{32b}, K. Hanagaki¹¹⁵, K. Hanawa¹⁵⁹, M. Hance¹⁴, C. Handel⁸⁰, P. Hanke^{58a}, J.R. Hansen³⁵, J.B. Hansen³⁵, J.D. Hansen³⁵, P.H. Hansen³⁵, P. Hansson¹⁴², K. Hara¹⁵⁹, G.A. Hare¹³⁶, T. Harenberg¹⁷³, S. Harkusha⁸⁹, D. Harper⁸⁶, R.D. Harrington⁴⁵, O.M. Harris¹³⁷, K. Harrison¹⁷, J. Hartert⁴⁸, F. Hartjes¹⁰⁴, T. Haruyama⁶⁵, A. Harvey⁵⁶, S. Hasegawa¹⁰⁰, Y. Hasegawa¹³⁹, S. Hassani¹³⁵, M. Hatch²⁹, D. Hauff⁹⁸, S. Haug¹⁶, M. Hauschild²⁹, R. Hauser⁸⁷, M. Havranek²⁰, B.M. Hawes¹¹⁷, C.M. Hawkes¹⁷, R.J. Hawkins²⁹, A.D. Hawkins⁷⁸, D. Hawkins¹⁶², T. Hayakawa⁶⁶, T. Hayashi¹⁵⁹, D. Hayden⁷⁵, H.S. Hayward⁷², S.J. Haywood¹²⁸, E. Hazen²¹, M. He^{32d}, S.J. Head¹⁷, V. Hedberg⁷⁸, L. Heelan⁷, S. Heim⁸⁷, B. Heinemann¹⁴, S. Heisterkamp³⁵, L. Helary⁴, C. Heller⁹⁷, M. Heller²⁹, S. Hellman^{145a,145b}, D. Hellmich²⁰, C. Helsens¹¹, R.C.W. Henderson⁷⁰, M. Henke^{58a}, A. Henrichs⁵⁴, A.M. Henriques Correia²⁹, S. Henrot-Versille¹¹⁴, F. Henry-Couannier⁸², C. Hensel⁵⁴, T. Henß¹⁷³, C.M. Hernandez⁷, Y. Hernández Jiménez¹⁶⁶, R. Herrberg¹⁵, A.D. Hershenhorn¹⁵¹, G. Herten⁴⁸, R. Hertenberger⁹⁷, L. Hervas²⁹, N.P. Hessey¹⁰⁴, E. Higón-Rodríguez¹⁶⁶, D. Hill^{5,*}, J.C. Hill²⁷, N. Hill⁵, K.H. Hiller⁴¹, S. Hillert²⁰, S.J. Hillier¹⁷, I. Hinchliffe¹⁴, E. Hines¹¹⁹, M. Hirose¹¹⁵, F. Hirsch⁴², D. Hirschbuehl¹⁷³, J. Hobbs¹⁴⁷, N. Hod¹⁵², M.C. Hodgkinson¹³⁸, P. Hodgson¹³⁸, A. Hoecker²⁹, M.R. Hoferkamp¹⁰², J. Hoffman³⁹, D. Hoffmann⁸², M. Hohlfeld⁸⁰, M. Holder¹⁴⁰, S.O. Holmgren^{145a}, T. Holy¹²⁶, J.L. Holzbauer⁸⁷, Y. Homma⁶⁶, T.M. Hong¹¹⁹, L. Hooft van Huysduynen¹⁰⁷, T. Horazdovsky¹²⁶, C. Horn¹⁴², S. Horner⁴⁸, J.-Y. Hostachy⁵⁵, S. Hou¹⁵⁰, M.A. Houlden⁷², A. Hoummada^{134a}, J. Howarth⁸¹, D.F. Howell¹¹⁷, I. Hristova¹⁵, J. Hrivnac¹¹⁴, I. Hruska¹²⁴, T. Hryn'ova⁴, P.J. Hsu⁸⁰, S.-C. Hsu¹⁴, G.S. Huang¹¹⁰, Z. Hubacek¹²⁶, F. Hubaut⁸², F. Huegging²⁰, A. Huettmann⁴¹, T.B. Huffman¹¹⁷, E.W. Hughes³⁴, G. Hughes⁷⁰, R.E. Hughes-Jones⁸¹, M. Huhtinen²⁹, P. Hurst⁵⁷, M. Hurwitz¹⁴, U. Husemann⁴¹, N. Huseynov^{64,p}, J. Huston⁸⁷, J. Huth⁵⁷, G. Iacobucci⁴⁹, G. Iakovidis⁹, M. Ibbotson⁸¹, I. Ibragimov¹⁴⁰, R. Ichimiya⁶⁶, L. Iconomidou-Fayard¹¹⁴, J. Idarraga¹¹⁴, P. Iengo^{101a}, O. Igonkina¹⁰⁴, Y. Ikegami⁶⁵, M. Ikeno⁶⁵, Y. Ilchenko³⁹, D. Iliadis¹⁵³, N. Ilic¹⁵⁷, D. Imbault⁷⁷, M. Imori¹⁵⁴, T. Ince²⁰, J. Inigo-Golfín²⁹, P. Ioannou⁸, M. Iodice^{133a}, V. Ippolito^{131a,131b}, A. Irlles Quiles¹⁶⁶, C. Isaksson¹⁶⁵, A. Ishikawa⁶⁶, M. Ishino⁶⁷, R. Ishmukhametov³⁹, C. Issever¹¹⁷, S. Istin^{18a}, A.V. Ivashin¹²⁷, W. Iwanski³⁸, H. Iwasaki⁶⁵, J.M. Izen⁴⁰, V. Izzo^{101a}, B. Jackson¹¹⁹, J.N. Jackson⁷², P. Jackson¹⁴², M.R. Jaekel²⁹, V. Jain⁶⁰, K. Jakobs⁴⁸, S. Jakobsen³⁵, J. Jakubek¹²⁶, D.K. Jana¹¹⁰, E. Jankowski¹⁵⁷, E. Jansen⁷⁶, H. Jansen²⁹, A. Jantsch⁹⁸, M. Janus²⁰, G. Jarlskog⁷⁸, L. Jeanty⁵⁷, K. Jelen³⁷, I. Jen-La Plante³⁰, P. Jenni²⁹,

A. Jeremie⁴, P. Jež³⁵, S. Jézéquel⁴, M.K. Jha^{19a}, H. Ji¹⁷¹, W. Ji⁸⁰, J. Jia¹⁴⁷, Y. Jiang^{32b}, M. Jimenez Belenguer⁴¹, G. Jin^{32b}, S. Jin^{32a}, O. Jinnouchi¹⁵⁶, M.D. Joergensen³⁵, D. Joffe³⁹, L.G. Johansen¹³, M. Johansen^{145a,145b}, K.E. Johansson^{145a}, P. Johansson¹³⁸, S. Johnert⁴¹, K.A. Johns⁶, K. Jon-And^{145a,145b}, G. Jones⁸¹, R.W.L. Jones⁷⁰, T.W. Jones⁷⁶, T.J. Jones⁷², O. Jonsson²⁹, C. Joram²⁹, P.M. Jorge^{123a}, J. Joseph¹⁴, T. Jovin^{12b}, X. Ju¹⁷¹, C.A. Jung⁴², R.M. Jungst²⁹, V. Juraneck¹²⁴, P. Jussel⁶¹, A. Juste Rozas¹¹, V.V. Kabachenko¹²⁷, S. Kabana¹⁶, M. Kaci¹⁶⁶, A. Kaczmarska³⁸, P. Kadlecik³⁵, M. Kado¹¹⁴, H. Kagan¹⁰⁸, M. Kagan⁵⁷, S. Kaiser⁹⁸, E. Kajomovitz¹⁵¹, S. Kalinin¹⁷³, L.V. Kalinovskaya⁶⁴, S. Kama³⁹, N. Kanaya¹⁵⁴, M. Kaneda²⁹, S. Kaneti²⁷, T. Kanno¹⁵⁶, V.A. Kantserov⁹⁵, J. Kanzaki⁶⁵, B. Kaplan¹⁷⁴, A. Kapliy³⁰, J. Kaplon²⁹, D. Kar⁴³, M. Karagounis²⁰, M. Karagoz¹¹⁷, M. Karnevskiy⁴¹, K. Karr⁵, V. Kartvelishvili⁷⁰, A.N. Karyukhin¹²⁷, L. Kashif¹⁷¹, G. Kasieczka^{58b}, R.D. Kass¹⁰⁸, A. Kastanas¹³, M. Kataoka⁴, Y. Kataoka¹⁵⁴, E. Katsoufis⁹, J. Katzy⁴¹, V. Kaushik⁶, K. Kawagoe⁶⁶, T. Kawamoto¹⁵⁴, G. Kawamura⁸⁰, M.S. Kayl¹⁰⁴, V.A. Kazanin¹⁰⁶, M.Y. Kazarinov⁶⁴, R. Keeler¹⁶⁸, R. Kehoe³⁹, M. Keil⁵⁴, G.D. Kekelidze⁶⁴, J. Kennedy⁹⁷, C.J. Kenney¹⁴², M. Kenyon⁵³, O. Kepka¹²⁴, N. Kersch²⁹, B.P. Kerševan⁷³, S. Kersten¹⁷³, K. Kessoku¹⁵⁴, J. Keung¹⁵⁷, F. Khalil-zada¹⁰, H. Khandanyan¹⁶⁴, A. Khanov¹¹¹, D. Kharchenko⁶⁴, A. Khodinov⁹⁵, A.G. Kholodenko¹²⁷, A. Khomich^{58a}, T.J. Khoo²⁷, G. Khoriali²⁰, A. Khoroshilov¹⁷³, N. Khovanskiy⁶⁴, V. Khovanskiy⁹⁴, E. Khramov⁶⁴, J. Khubua^{51b}, H. Kim^{145a,145b}, M.S. Kim², P.C. Kim¹⁴², S.H. Kim¹⁵⁹, N. Kimura¹⁶⁹, O. Kind¹⁵, B.T. King⁷², M. King⁶⁶, R.S.B. King¹¹⁷, J. Kirk¹²⁸, L.E. Kirsch²², A.E. Kiryunin⁹⁸, T. Kishimoto⁶⁶, D. Kisielewska³⁷, T. Kittelmann¹²², A.M. Kiver¹²⁷, E. Kladiva^{143b}, J. Klaiber-Lodewigs⁴², M. Klein⁷², U. Klein⁷², K. Kleinknecht⁸⁰, M. Klemetti⁸⁴, A. Klier¹⁷⁰, P. Klimek^{145a,145b}, A. Klimentov²⁴, R. Klingenberg⁴², J.A. Klinger⁸¹, E.B. Klinkby³⁵, T. Klioutchnikova²⁹, P.F. Klok¹⁰³, S. Klous¹⁰⁴, E.-E. Kluge^{58a}, T. Kluge⁷², P. Kluit¹⁰⁴, S. Kluth⁹⁸, N.S. Knecht¹⁵⁷, E. Kneringer⁶¹, J. Knobloch²⁹, E.B.F.G. Knoops⁸², A. Knue⁵⁴, B.R. Ko⁴⁴, T. Kobayashi¹⁵⁴, M. Kobel⁴³, M. Kocian¹⁴², P. Kodys¹²⁵, K. Köneke²⁹, A.C. König¹⁰³, S. Koenig⁸⁰, L. Köpke⁸⁰, F. Koetsveld¹⁰³, P. Koesvarki²⁰, T. Koffas²⁸, E. Koffeman¹⁰⁴, L.A. Kogan¹¹⁷, F. Kohn⁵⁴, Z. Kohout¹²⁶, T. Kohriki⁶⁵, T. Koi¹⁴², T. Kokott²⁰, G.M. Kolachev¹⁰⁶, H. Kolanoski¹⁵, V. Kolesnikov⁶⁴, I. Koletsou^{88a}, J. Koll⁸⁷, D. Kollar²⁹, M. Kollfrath⁴⁸, S.D. Kolya⁸¹, A.A. Komar⁹³, Y. Komori¹⁵⁴, T. Kondo⁶⁵, T. Kono^{41,q}, A.I. Kononov⁴⁸, R. Konoplich^{107,r}, N. Konstantinidis⁷⁶, A. Kootz¹⁷³, S. Koperny³⁷, K. Korcyl³⁸, K. Kordas¹⁵³, V. Koreshev¹²⁷, A. Korn¹¹⁷, A. Korol¹⁰⁶, I. Korolkov¹¹, E.V. Korolkova¹³⁸, V.A. Korotkov¹²⁷, O. Kortner⁹⁸, S. Kortner⁹⁸, V.V. Kostyukhin²⁰, M.J. Kotamäki²⁹, S. Kotov⁹⁸, V.M. Kotov⁶⁴, A. Kotwal⁴⁴, C. Kourkoumelis⁸, V. Kouskoura¹⁵³, A. Koutsman^{158a}, R. Kowalewski¹⁶⁸, T.Z. Kowalski³⁷, W. Kozanecki¹³⁵, A.S. Kozhin¹²⁷, V. Kral¹²⁶, V.A. Kramarenko⁹⁶, G. Kramberger⁷³, M.W. Krasny⁷⁷, A. Krasznahorkay¹⁰⁷, J. Kraus⁸⁷, J.K. Kraus²⁰, A. Kreisel¹⁵², F. Krejci¹²⁶, J. Kretzschmar⁷², N. Krieger⁵⁴, P. Krieger¹⁵⁷, K. Kroeninger⁵⁴, H. Kroha⁹⁸, J. Kroll¹¹⁹, J. Kroseberg²⁰, J. Krstic^{12a}, U. Kruchonak⁶⁴, H. Krüger²⁰, T. Kruker¹⁶, N. Krumnack⁶³, Z.V. Krumshteyn⁶⁴, A. Kruth²⁰, T. Kubota⁸⁵, S. Kuehn⁴⁸, A. Kugel^{58c}, T. Kuhl⁴¹, D. Kuhn⁶¹, V. Kukhtin⁶⁴, Y. Kulchitsky⁸⁹, S. Kuleshov^{31b}, C. Kummer⁹⁷, M. Kuna⁷⁷, N. Kundu¹¹⁷, J. Kunkle¹¹⁹, A. Kupco¹²⁴, H. Kurashige⁶⁶, M. Kurata¹⁵⁹, Y.A. Kurochkin⁸⁹, V. Kus¹²⁴, E.S. Kuwertz¹⁴⁶, M. Kuze¹⁵⁶, J. Kvita¹⁴¹, R. Kwee¹⁵, A. La Rosa⁴⁹, L. La Rotonda^{36a,36b}, L. Labarga⁷⁹, J. Labbe⁴, S. Lablak^{134a}, C. Lacasta¹⁶⁶, F. Lacava^{131a,131b}, H. Lacker¹⁵, D. Lacour⁷⁷, V.R. Lacuesta¹⁶⁶, E. Ladygin⁶⁴, R. Lafaye⁴, B. Laforge⁷⁷, T. Lagouri⁷⁹, S. Lai⁴⁸, E. Laisne⁵⁵, M. Lamanna²⁹, C.L. Lampen⁶, W. Lampl⁶, E. Lancon¹³⁵, U. Landgraf⁴⁸, M.P.J. Landon⁷⁴, H. Landsman¹⁵¹, J.L. Lane⁸¹, C. Lange⁴¹, A.J. Lankford¹⁶², F. Lanni²⁴, K. Lantzsch¹⁷³, S. Laplace⁷⁷, C. Lapoire²⁰, J.F. Laporte¹³⁵, T. Lari^{88a}, A.V. Larionov¹²⁷, A. Larner¹¹⁷, C. Lasseur²⁹, M. Lassnig²⁹, P. Laurelli⁴⁷, W. Lavrijsen¹⁴, P. Laycock⁷², A.B. Lazarev⁶⁴, O. Le Dortz⁷⁷, E. Le Guirrec⁸², C. Le Maner¹⁵⁷, E. Le Menedeu⁹, C. Lebel⁹², T. LeCompte⁵, F. Ledroit-Guillon⁵⁵, H. Lee¹⁰⁴, J.S.H. Lee¹¹⁵, S.C. Lee¹⁵⁰, L. Lee¹⁷⁴, M. Lefebvre¹⁶⁸, M. Legendre¹³⁵, A. Leger⁴⁹, B.C. LeGeyt¹¹⁹, F. Legger⁹⁷, C. Leggett¹⁴, M. Lehmacher²⁰, G. Lehmann Miotto²⁹, X. Lei⁶, M.A.L. Leite^{23d}, R. Leitner¹²⁵, D. Lellouch¹⁷⁰, M. Leltchouk³⁴, B. Lemmer⁵⁴, V. Lendermann^{58a}, K.J.C. Leney^{144b}, T. Lenz¹⁰⁴, G. Lenzen¹⁷³, B. Lenzi²⁹, K. Leonhardt⁴³, S. Leontsinis⁹, C. Leroy⁹², J.-R. Lessard¹⁶⁸, J. Lesser^{145a}, C.G. Lester²⁷, A. Leung Fook Cheong¹⁷¹, J. Levêque⁴, D. Levin⁸⁶, L.J. Levinson¹⁷⁰, M.S. Levitski¹²⁷, A. Lewis¹¹⁷, G.H. Lewis¹⁰⁷, A.M. Leyko²⁰, M. Leyton¹⁵, B. Li⁸², H. Li^{171,s}, S. Li^{32b,t}, X. Li⁸⁶, Z. Liang^{117,u}, H. Liao³³, B. Liberti^{132a}, P. Lichard²⁹, M. Lichtnecker⁹⁷, K. Lie¹⁶⁴, W. Liebig¹³, R. Lifshitz¹⁵¹, C. Limbach²⁰, A. Limosani⁸⁵, M. Limper⁶², S.C. Lin^{150,v}, F. Linde¹⁰⁴, J.T. Linnemann⁸⁷, E. Lipeles¹¹⁹, L. Lipinsky¹²⁴, A. Lipniacka¹³, T.M. Liss¹⁶⁴, D. Lissauer²⁴, A. Lister⁴⁹, A.M. Litke¹³⁶, C. Liu²⁸, D. Liu¹⁵⁰, H. Liu⁸⁶, J.B. Liu⁸⁶, M. Liu^{32b}, S. Liu², Y. Liu^{32b}, M. Livan^{118a,118b}, S.S.A. Livermore¹¹⁷, A. Lleres⁵⁵, J. Llorente Merino⁷⁹, S.L. Lloyd⁷⁴, E. Lobodzinska⁴¹, P. Loch⁶, W.S. Lockman¹³⁶, T. Loddenkoetter²⁰, F.K. Loebinger⁸¹, A. Loginov¹⁷⁴, C.W. Loh¹⁶⁷, T. Lohse¹⁵, K. Lohwasser⁴⁸, M. Lokajicek¹²⁴, J. Loken¹¹⁷, V.P. Lombardo⁴, R.E. Long⁷⁰, L. Lopes^{123a}, D. Lopez Mateos⁵⁷, J. Lorenz⁹⁷, M. Losada¹⁶¹, P. Loscutoff¹⁴, F. Lo Sterzo^{131a,131b}, M.J. Losty^{158a}, X. Lou⁴⁰, A. Lounis¹¹⁴, K.F. Loureiro¹⁶¹, J. Love²¹, P.A. Love⁷⁰, A.J. Lowe^{142,e}, F. Lu^{32a}, H.J. Lubatti¹³⁷, C. Luci^{131a,131b}, A. Lucotte⁵⁵, A. Ludwig⁴³, D. Ludwig⁴¹, I. Ludwig⁴⁸, J. Ludwig⁴⁸, F. Luehring⁶⁰, G. Luijckx¹⁰⁴, D. Lumb⁴⁸, L. Luminari^{131a}, E. Lund¹¹⁶, B. Lund-Jensen¹⁴⁶, B. Lundberg⁷⁸, J. Lundberg^{145a,145b}, J. Lundquist³⁵, M. Lungwitz⁸⁰, G. Lutz⁹⁸, D. Lynn²⁴, J. Lys¹⁴, E. Lytken⁷⁸, H. Ma²⁴, L.L. Ma¹⁷¹, J.A. Macana Goia⁹², G. Maccarrone⁴⁷, A. Macchiolo⁹⁸, B. Maček⁷³, J. Machado Miguens^{123a}, R. Mackeprang³⁵, R.J. Madaras¹⁴,

W.F. Mader⁴³, R. Maenner^{58c}, T. Maeno²⁴, P. Mättig¹⁷³, S. Mättig⁴¹, L. Magnoni²⁹, E. Magradze⁵⁴, Y. Mahalalel¹⁵², K. Mahboubi⁴⁸, G. Mahout¹⁷, C. Maiani^{131a,131b}, C. Maidantchik^{23a}, A. Maio^{123a,b}, S. Majewski²⁴, Y. Makida⁶⁵, N. Makovec¹¹⁴, P. Mal¹³⁵, B. Malaescu²⁹, Pa. Malecki³⁸, P. Malecki³⁸, V.P. Maleev¹²⁰, F. Malek⁵⁵, U. Mallik⁶², D. Malon⁵, C. Malone¹⁴², S. Maltezos⁹, V. Malyshev¹⁰⁶, S. Malyukov²⁹, R. Mameghani⁹⁷, J. Mamuzic^{12b}, A. Manabe⁶⁵, L. Mandelli^{88a}, I. Mandić⁷³, R. Mandrysch¹³⁶, J. Maneira^{123a}, P.S. Mangedard⁸⁷, L. Manhaes de Andrade Filho^{23a}, I.D. Manjavidze⁶⁴, A. Mann⁵⁴, P.M. Manning¹³⁶, A. Manousakis-Katsikakis⁸, B. Mansoulie¹³⁵, A. Manz⁹⁸, A. Mapelli²⁹, L. Mapelli²⁹, L. March⁷⁹, J.F. Marchand²⁸, F. Marchese^{132a,132b}, G. Marchiori⁷⁷, M. Marcisovsky¹²⁴, A. Marin^{21,*}, C.P. Marino¹⁶⁸, F. Marroquim^{23a}, R. Marshall⁸¹, Z. Marshall²⁹, F.K. Martens¹⁵⁷, S. Marti-Garcia¹⁶⁶, A.J. Martin¹⁷⁴, B. Martin²⁹, B. Martin⁸⁷, F.F. Martin¹¹⁹, J.P. Martin⁹², Ph. Martin⁵⁵, T.A. Martin¹⁷, V.J. Martin⁴⁵, B. Martin dit Latour⁴⁹, S. Martin-Haugh¹⁴⁸, M. Martinez¹¹, V. Martinez Outschoorn⁵⁷, A.C. Martyniuk¹⁶⁸, M. Marx⁸¹, F. Marzano^{131a}, A. Marzin¹¹⁰, L. Masetti⁸⁰, T. Mashimo¹⁵⁴, R. Mashinistov⁹³, J. Masik⁸¹, A.L. Maslennikov¹⁰⁶, I. Massa^{19a,19b}, G. Massaro¹⁰⁴, N. Massol⁴, P. Mastrandrea^{131a,131b}, A. Mastroberardino^{36a,36b}, T. Masubuchi¹⁵⁴, M. Mathes²⁰, P. Matricon¹¹⁴, H. Matsumoto¹⁵⁴, H. Matsunaga¹⁵⁴, T. Matsushita⁶⁶, C. Matzavali^{117,c}, J.M. Maugain²⁹, J. Maurer⁸², S.J. Maxfield⁷², D.A. Maximov^{106,f}, E.N. May⁵, A. Mayne¹³⁸, R. Mazini¹⁵⁰, M. Mazur²⁰, M. Mazzanti^{88a}, E. Mazzoni^{121a,121b}, S.P. Mc Kee⁸⁶, A. McCann¹⁶⁴, R.L. McCarthy¹⁴⁷, T.G. McCarthy²⁸, N.A. McCubbin¹²⁸, K.W. McFarlane⁵⁶, J.A. McFayden¹³⁸, H. McGlone⁵³, G. Mchedlidze^{51b}, R.A. McLaren²⁹, T. McLaughlan¹⁷, S.J. McMahon¹²⁸, R.A. McPherson^{168,j}, A. Meade⁸³, J. Mechnich¹⁰⁴, M. Mechtel¹⁷³, M. Medinnis⁴¹, R. Meera-Lebbai¹¹⁰, T. Meguro¹¹⁵, R. Mehdiev⁹², S. Mehlhase³⁵, A. Mehta⁷², K. Meier^{58a}, B. Meirose⁷⁸, C. Melachrinou³⁰, B.R. Mellado Garcia¹⁷¹, L. Mendoza Navas¹⁶¹, Z. Meng^{150,s}, A. Mengarelli^{19a,19b}, S. Menke⁹⁸, C. Menot²⁹, E. Meoni¹¹, K.M. Mercurio⁵⁷, P. Mermod⁴⁹, L. Merola^{101a,101b}, C. Meroni^{88a}, F.S. Merritt³⁰, A. Messina²⁹, J. Metcalfe¹⁰², A.S. Mete⁶³, C. Meyer⁸⁰, C. Meyer³⁰, J-P. Meyer¹³⁵, J. Meyer¹⁷², J. Meyer⁵⁴, T.C. Meyer²⁹, W.T. Meyer⁶³, J. Miao^{32d}, S. Michal²⁹, L. Micu^{25a}, R.P. Middleton¹²⁸, S. Migas⁷², L. Mijović⁴¹, G. Mikenberg¹⁷⁰, M. Mikestikova¹²⁴, M. Mikuž⁷³, D.W. Miller³⁰, R.J. Miller⁸⁷, W.J. Mills¹⁶⁷, C. Mills⁵⁷, A. Milov¹⁷⁰, D.A. Milstead^{145a,145b}, D. Milstein¹⁷⁰, A.A. Minaenko¹²⁷, M. Miñano Moya¹⁶⁶, I.A. Minashvili⁶⁴, A.I. Mincer¹⁰⁷, B. Mindur³⁷, M. Mineev⁶⁴, Y. Ming¹⁷¹, L.M. Mir¹¹, G. Mirabelli^{131a}, L. Miralles Verge¹¹, A. Misiejuk⁷⁵, J. Mitrevski¹³⁶, G.Y. Mitrofanov¹²⁷, V.A. Mitsou¹⁶⁶, S. Mitsui⁶⁵, P.S. Miyagawa¹³⁸, K. Miyazaki⁶⁶, J.U. Mjörnmark⁷⁸, T. Moa^{145a,145b}, P. Mockett¹³⁷, S. Moed⁵⁷, V. Moeller²⁷, K. Mönig⁴¹, N. Möser²⁰, S. Mohapatra¹⁴⁷, W. Mohr⁴⁸, S. Mohr dieck-Möck⁹⁸, A.M. Moiseev^{127,*}, R. Moles-Valls¹⁶⁶, J. Molina-Perez²⁹, J. Monk⁷⁶, E. Monnier⁸², S. Montesano^{88a,88b}, F. Monticelli⁶⁹, S. Monzani^{19a,19b}, R.W. Moore², G.F. Moorhead⁸⁵, C. Mora Herrera⁴⁹, A. Moraes⁵³, N. Morange¹³⁵, J. Morel⁵⁴, G. Morello^{36a,36b}, D. Moreno⁸⁰, M. Moreno Llacer¹⁶⁶, P. Morettini^{50a}, M. Morii⁵⁷, J. Morin⁷⁴, A.K. Morley²⁹, G. Mornacchi²⁹, S.V. Morozov⁹⁵, J.D. Morris⁷⁴, L. Morvaj¹⁰⁰, H.G. Moser⁹⁸, M. Mosidze^{51b}, J. Moss¹⁰⁸, R. Mount¹⁴², E. Mountricha^{9,w}, S.V. Mouraviev⁹³, E.J.W. Moyses⁸³, M. Mudrinic^{12b}, F. Mueller^{58a}, J. Mueller¹²², K. Mueller²⁰, T.A. Müller⁹⁷, T. Mueller⁸⁰, D. Muenstermann²⁹, A. Muir¹⁶⁷, Y. Munwes¹⁵², W.J. Murray¹²⁸, I. Mussche¹⁰⁴, E. Musto^{101a,101b}, A.G. Myagkov¹²⁷, M. Myska¹²⁴, J. Nadal¹¹, K. Nagai¹⁵⁹, K. Nagano⁶⁵, Y. Nagasaka⁵⁹, M. Nagel⁹⁸, A.M. Nairz²⁹, Y. Nakahama²⁹, K. Nakamura¹⁵⁴, T. Nakamura¹⁵⁴, I. Nakano¹⁰⁹, G. Nanava²⁰, A. Napier¹⁶⁰, R. Narayan^{58b}, M. Nash^{76,c}, N.R. Nation²¹, T. Nattermann²⁰, T. Naumann⁴¹, G. Navarro¹⁶¹, H.A. Neal⁸⁶, E. Nebot⁷⁹, P.Yu. Nechaeva⁹³, T.J. Neep⁸¹, A. Negri^{118a,118b}, G. Negri²⁹, S. Nektarijevic⁴⁹, A. Nelson¹⁶², S. Nelson¹⁴², T.K. Nelson¹⁴², S. Nemecek¹²⁴, P. Nemethy¹⁰⁷, A.A. Nepomuceno^{23a}, M. Nessi^{29,x}, M.S. Neubauer¹⁶⁴, A. Neusiedl⁸⁰, R.M. Neves¹⁰⁷, P. Nevski²⁴, P.R. Newman¹⁷, V. Nguyen Thi Hong¹³⁵, R.B. Nickerson¹¹⁷, R. Nicolaidou¹³⁵, L. Nicolas¹³⁸, B. Nicquevert²⁹, F. Niedercorn¹¹⁴, J. Nielsen¹³⁶, T. Niinikoski²⁹, N. Nikiforou³⁴, A. Nikiforov¹⁵, V. Nikolaenko¹²⁷, K. Nikolaev⁶⁴, I. Nikolic-Audit⁷⁷, K. Nikolics⁴⁹, K. Nikolopoulos²⁴, H. Nilsen⁴⁸, P. Nilsson⁷, Y. Ninomiya¹⁵⁴, A. Nisati^{131a}, T. Nishiyama⁶⁶, R. Nisius⁹⁸, L. Nodulman⁵, M. Nomachi¹¹⁵, I. Nomidis¹⁵³, M. Nordberg²⁹, B. Nordkvist^{145a,145b}, P.R. Norton¹²⁸, J. Novakova¹²⁵, M. Nozaki⁶⁵, L. Nozka¹¹², I.M. Nugent^{158a}, A.-E. Nuncio-Quiroz²⁰, G. Nunes Hanninger⁸⁵, T. Nunnemann⁹⁷, E. Nurse⁷⁶, T. Nyman²⁹, B.J. O'Brien⁴⁵, S.W. O'Neale^{17,*}, D.C. O'Neil¹⁴¹, V. O'Shea⁵³, L.B. Oakes⁹⁷, F.G. Oakham^{28,d}, H. Oberlack⁹⁸, J. Ocariz⁷⁷, A. Ochi⁶⁶, S. Oda¹⁵⁴, S. Odaka⁶⁵, J. Odier⁸², H. Ogren⁶⁰, A. Oh⁸¹, S.H. Oh⁴⁴, C.C. Ohm^{145a,145b}, T. Ohshima¹⁰⁰, H. Ohshita¹³⁹, T. Ohsugi¹⁷⁷, S. Okada⁶⁶, H. Okawa¹⁶², Y. Okumura¹⁰⁰, T. Okuyama¹⁵⁴, A. Olariu^{25a}, M. Olcese^{50a}, A.G. Olchevski⁶⁴, M. Oliveira^{123a,h}, D. Oliveira Damazio²⁴, E. Oliver Garcia¹⁶⁶, D. Olivito¹¹⁹, A. Olszewski³⁸, J. Olszowska³⁸, C. Omachi⁶⁶, A. Onofre^{123a,y}, P.U.E. Onyisi³⁰, C.J. Oram^{158a}, M.J. Oreglia³⁰, Y. Oren¹⁵², D. Orestano^{133a,133b}, I. Orlov¹⁰⁶, C. Oropeza Barrera⁵³, R.S. Orr¹⁵⁷, B. Osculati^{50a,50b}, R. Ospanov¹¹⁹, C. Osuna¹¹, G. Otero y Garzon²⁶, J.P. Ottersbach¹⁰⁴, M. Ouchrif^{134d}, E.A. Ouellette¹⁶⁸, F. Ould-Saada¹¹⁶, A. Ouraou¹³⁵, Q. Ouyang^{32a}, A. Ovcharova¹⁴, M. Owen⁸¹, S. Owen¹³⁸, V.E. Ozcan^{18a}, N. Ozturk⁷, A. Pacheco Pages¹¹, C. Padilla Aranda¹¹, S. Pagan Griso¹⁴, E. Paganis¹³⁸, F. Paige²⁴, P. Pais⁸³, K. Pajchel¹¹⁶, G. Palacino^{158b}, C.P. Palestini⁶, S. Palestini²⁹, D. Pallin³³, A. Palma^{123a}, J.D. Palmer¹⁷, Y.B. Pan¹⁷¹, E. Panagiotopoulou⁹, B. Panes^{31a}, N. Panikashvili⁸⁶, S. Panitkin²⁴, D. Pantea^{25a}, M. Panuskova¹²⁴, V. Paolone¹²², A. Papadellis^{145a}, Th.D. Papadopoulou⁹, A. Paramonov⁵, W. Park^{24,z}, M.A. Parker²⁷, F. Parodi^{50a,50b}, J.A. Parsons³⁴, U. Parzefall⁴⁸, E. Pasqualucci^{131a}, S. Passaggio^{50a}, A. Passeri^{133a}, F. Pastore^{133a,133b}, Fr. Pas-

tore⁷⁵, G. Pásztor^{49,aa}, S. Pataraiia¹⁷³, N. Patel¹⁴⁹, J.R. Pater⁸¹, S. Patricelli^{101a,101b}, T. Pauly²⁹, M. Pecsý^{143a}, M.I. Pedraza Morales¹⁷¹, S.V. Peleganchuk¹⁰⁶, H. Peng^{32b}, R. Pengo²⁹, A. Penson³⁴, J. Penwell⁶⁰, M. Perantoni^{23a}, K. Perez^{34,ab}, T. Perez Cavalcanti⁴¹, E. Perez Codina¹¹, M.T. Pérez García-Estañ¹⁶⁶, V. Perez Reale³⁴, L. Perini^{88a,88b}, H. Pernegger²⁹, R. Perrino^{71a}, P. Perrodo⁴, S. Persema^{3a}, A. Perus¹¹⁴, V.D. Peshekhonov⁶⁴, K. Peters²⁹, B.A. Petersen²⁹, J. Petersen²⁹, T.C. Petersen³⁵, E. Petit⁴, A. Petridis¹⁵³, C. Petridou¹⁵³, E. Petrolo^{131a}, F. Petrucci^{133a,133b}, D. Petschull⁴¹, M. Petteni¹⁴¹, R. Pezoa^{31b}, A. Phan⁸⁵, P.W. Phillips¹²⁸, G. Piacquadio²⁹, E. Piccaro⁷⁴, M. Piccinini^{19a,19b}, S.M. Piec⁴¹, R. Piegaiia²⁶, D.T. Pignotti¹⁰⁸, J.E. Pilcher³⁰, A.D. Pilkington⁸¹, J. Pina^{123a,b}, M. Pinamonti^{163a,163c}, A. Pinder¹¹⁷, J.L. Pinfold², J. Ping^{32c}, B. Pinto^{123a}, O. Pirotte²⁹, C. Pizio^{88a,88b}, M. Plamondon¹⁶⁸, M.-A. Pleier²⁴, A.V. Pleskach¹²⁷, A. Poblaguev²⁴, S. Poddar^{58a}, F. Podlyski³³, L. Poggioli¹¹⁴, T. Poghosyan²⁰, M. Pohl⁴⁹, F. Polci⁵⁵, G. Polesello^{118a}, A. Policicchio^{36a,36b}, A. Polini^{19a}, J. Poll⁷⁴, V. Polychronakos²⁴, D.M. Pomarede¹³⁵, D. Pomeroy²², K. Pommès²⁹, L. Pontecorvo^{131a}, B.G. Pope⁸⁷, G.A. Popeneciu^{25a}, D.S. Popovic^{12a}, A. Poppleton²⁹, X. Portell Bueso²⁹, C. Posch²¹, G.E. Pospelov⁹⁸, S. Pospisil¹²⁶, I.N. Potrap⁹⁸, C.J. Potter¹⁴⁸, C.T. Potter¹¹³, G. Poulard²⁹, J. Poveda¹⁷¹, R. Prabhu⁷⁶, P. Pralavorio⁸², A. Pranko¹⁴, S. Prasad⁵⁷, R. Pravahan⁷, S. Prell⁶³, K. Pretzl¹⁶, L. Pribyl²⁹, D. Price⁶⁰, J. Price⁷², L.E. Price⁵, M.J. Price²⁹, D. Prieur¹²², M. Primavera^{71a}, K. Prokofiev¹⁰⁷, F. Prokoshin^{31b}, S. Protopopescu²⁴, J. Proudfoot⁵, X. Prudent⁴³, M. Przybycien³⁷, H. Przysieszniak⁴, S. Psoroulas²⁰, E. Ptacek¹¹³, E. Pueschel⁸³, J. Purdham⁸⁶, M. Purohit^{24,z}, P. Puzo¹¹⁴, Y. Pylypchenko⁶², J. Qian⁸⁶, Z. Qian⁸², Z. Qin⁴¹, A. Quadt⁵⁴, D.R. Quarrie¹⁴, W.B. Quayle¹⁷¹, F. Quinonez^{31a}, M. Raas¹⁰³, V. Radescu^{58b}, B. Radics²⁰, P. Radloff¹¹³, T. Rador^{18a}, F. Ragusa^{88a,88b}, G. Rahal¹⁷⁶, A.M. Rahimi¹⁰⁸, D. Rahm²⁴, S. Rajagopalan²⁴, M. Rammensee⁴⁸, M. Rammes¹⁴⁰, A.S. Randle-Conde³⁹, K. Randrianarivony²⁸, P.N. Ratoff⁷⁰, F. Rauscher⁹⁷, M. Raymond²⁹, A.L. Read¹¹⁶, D.M. Rebuffi^{118a,118b}, A. Redelbach¹⁷², G. Redlinger²⁴, R. Reece¹¹⁹, K. Reeves⁴⁰, A. Reichold¹⁰⁴, E. Reinherz-Aronis¹⁵², A. Reinsch¹¹³, I. Reisinger⁴², D. Reljic^{12a}, C. Rembser²⁹, Z.L. Ren¹⁵⁰, A. Renaud¹¹⁴, P. Renkel³⁹, M. Rescigno^{131a}, S. Resconi^{88a}, B. Resende¹³⁵, P. Reznicek⁹⁷, R. Rezvani¹⁵⁷, A. Richards⁷⁶, R. Richter⁹⁸, E. Richter-Was^{4,ac}, M. Ridel⁷⁷, M. Rijpstra¹⁰⁴, M. Rijssenbeek¹⁴⁷, A. Rimoldi^{118a,118b}, L. Rinaldi^{19a}, R.R. Rios³⁹, I. Riu¹¹, G. Rivoltella^{88a,88b}, F. Rizatdinova¹¹¹, E. Rizvi⁷⁴, S.H. Robertson^{84,j}, A. Robichaud-Veronneau¹¹⁷, D. Robinson²⁷, J.E.M. Robinson⁷⁶, M. Robinson¹¹³, A. Robson⁵³, J.G. Rocha de Lima¹⁰⁵, C. Roda^{121a,121b}, D. Roda Dos Santos²⁹, D. Rodriguez¹⁶¹, A. Roe⁵⁴, S. Roe²⁹, O. Røhne¹¹⁶, V. Rojo¹, S. Rolli¹⁶⁰, A. Romaniouk⁹⁵, M. Romano^{19a,19b}, V.M. Romanov⁶⁴, G. Romeo²⁶, E. Romero Adam¹⁶⁶, L. Roos⁷⁷, E. Ros¹⁶⁶, S. Rosati^{131a}, K. Rosbach⁴⁹, A. Rose¹⁴⁸, M. Rose⁷⁵, G.A. Rosenbaum¹⁵⁷, E.I. Rosenberg⁶³, P.L. Rosendahl¹³, O. Rosenthal¹⁴⁰, L. Rosselet⁴⁹, V. Rossetti¹¹, E. Rossi^{131a,131b}, L.P. Rossi^{50a}, M. Rotaru^{25a}, I. Roth¹⁷⁰, J. Rothberg¹³⁷, D. Rousseau¹¹⁴, C.R. Royon¹³⁵, A. Rozanov⁸², Y. Rozen¹⁵¹, X. Ruan^{114,ad}, I. Rubinskiy⁴¹, B. Ruckert⁹⁷, N. Ruckstuhl¹⁰⁴, V.I. Rud⁹⁶, C. Rudolph⁴³, G. Rudolph⁶¹, F. Rühr⁶, F. Ruggieri^{133a,133b}, A. Ruiz-Martinez⁶³, V. Rumiantsev^{90,*}, L. Rumyantsev⁶⁴, K. Runge⁴⁸, Z. Rurikova⁴⁸, N.A. Rusakovich⁶⁴, D.R. Rust⁶⁰, J.P. Rutherford⁶, C. Ruwiedel¹⁴, P. Ruzicka¹²⁴, Y.F. Ryabov¹²⁰, V. Ryadovikov¹²⁷, P. Ryan⁸⁷, M. Rybar¹²⁵, G. Rybkin¹¹⁴, N.C. Ryder¹¹⁷, S. Rzaeva¹⁰, A.F. Saavedra¹⁴⁹, I. Sadeh¹⁵², H.F.-W. Sadrozinski¹³⁶, R. Sadykov⁶⁴, F. Safai Tehrani^{131a}, H. Sakamoto¹⁵⁴, G. Salamanna⁷⁴, A. Salamon^{132a}, M. Saleem¹¹⁰, D. Salihagic⁹⁸, A. Salnikov¹⁴², J. Salt¹⁶⁶, B.M. Salvachua Ferrando⁵, D. Salvatore^{36a,36b}, F. Salvatore¹⁴⁸, A. Salvucci¹⁰³, A. Salzburger²⁹, D. Sampsonidis¹⁵³, B.H. Samset¹¹⁶, A. Sanchez^{101a,101b}, H. Sandaker¹³, H.G. Sander⁸⁰, M.P. Sanders⁹⁷, M. Sandhoff¹⁷³, T. Sandoval²⁷, C. Sandoval¹⁶¹, R. Sandstroem⁹⁸, S. Sandvoss¹⁷³, D.P.C. Sankey¹²⁸, A. Sansoni⁴⁷, C. Santamarina Rios⁸⁴, C. Santoni³³, R. Santonico^{132a,132b}, H. Santos^{123a}, J.G. Saraiva^{123a}, T. Sarangi¹⁷¹, E. Sarkisyan-Grinbaum⁷, F. Sarri^{121a,121b}, G. Sartisohn¹⁷³, O. Sasaki⁶⁵, N. Sasao⁶⁷, I. Satsounkevitch⁸⁹, G. Sauvage⁴, E. Sauvan⁴, J.B. Sauvan¹¹⁴, P. Savard^{157,d}, V. Savinov¹²², D.O. Savu²⁹, L. Sawyer^{24,1}, D.H. Saxon⁵³, L.P. SAYS³³, C. Sbarra^{19a}, A. Sbrizzi^{19a,19b}, O. Scallan⁹², D.A. Scannicchio¹⁶², M. Scarcella¹⁴⁹, J. Schaarschmidt¹¹⁴, P. Schacht⁹⁸, U. Schäfer⁸⁰, S. Schaepe²⁰, S. Schaezel^{58b}, A.C. Schaffer¹¹⁴, D. Schaile⁹⁷, R.D. Schamberger¹⁴⁷, A.G. Schamov¹⁰⁶, V. Scharf^{58a}, V.A. Schegelsky¹²⁰, D. Scheirich⁸⁶, M. Schernau¹⁶², M.I. Scherzer³⁴, C. Schiavi^{50a,50b}, J. Schieck⁹⁷, M. Schioppa^{36a,36b}, S. Schlenker²⁹, J.L. Schlereth⁵, E. Schmidt⁴⁸, K. Schmieden²⁰, C. Schmitt⁸⁰, S. Schmitt^{58b}, M. Schmitz²⁰, A. Schönig^{58b}, M. Schott²⁹, D. Schouten^{158a}, J. Schovancova¹²⁴, M. Schram⁸⁴, C. Schroeder⁸⁰, N. Schroer^{58c}, S. Schuh²⁹, G. Schuler²⁹, J. Schultes¹⁷³, H.-C. Schultz-Coulon^{58a}, H. Schulz¹⁵, J.W. Schumacher²⁰, M. Schumacher⁴⁸, B.A. Schumm¹³⁶, Ph. Schune¹³⁵, C. Schwanenberger⁸¹, A. Schwartzman¹⁴², Ph. Schwemling⁷⁷, R. Schwienhorst⁸⁷, R. Schwierz⁴³, J. Schwindling¹³⁵, T. Schwintz²⁰, M. Schwoerer⁴, W.G. Scott¹²⁸, J. Searcy¹¹³, G. Sedov⁴¹, E. Sedykh¹²⁰, E. Segura¹¹, S.C. Seidel¹⁰², A. Seiden¹³⁶, F. Seifert⁴³, J.M. Seixas^{23a}, G. Sekhniaidze^{101a}, K.E. Selbach⁴⁵, D.M. Seliverstov¹²⁰, B. Sellden^{145a}, G. Sellers⁷², M. Seman^{143b}, N. Semprini-Cesari^{19a,19b}, C. Serfon⁹⁷, L. Serin¹¹⁴, L. Serkin⁵⁴, R. Seuster⁹⁸, H. Severini¹¹⁰, M.E. Seviour⁸⁵, A. Sfyrila²⁹, E. Shabalina⁵⁴, M. Shamim¹¹³, L.Y. Shan^{32a}, J.T. Shank²¹, Q.T. Shao⁸⁵, M. Shapiro¹⁴, P.B. Shatalov⁹⁴, L. Shaver⁶, K. Shaw^{163a,163c}, D. Sherman¹⁷⁴, P. Sherwood⁷⁶, A. Shibata¹⁰⁷, H. Shichi¹⁰⁰, S. Shimizu²⁹, M. Shimojima⁹⁹, T. Shin⁵⁶, M. Shiyakova⁶⁴, A. Shmeleva⁹³, M.J. Shochet³⁰, D. Short¹¹⁷, S. Shrestha⁶³, M.A. Shupe⁶, P. Sicho¹²⁴, A. Sidoti^{131a}, F. Siegert⁴⁸, Dj. Sijacki^{12a}, O. Silbert¹⁷⁰, J. Silva^{123a,b}, Y. Silver¹⁵², D. Silverstein¹⁴², S.B. Silverstein^{145a}, V. Simak¹²⁶, O. Simard¹³⁵, Lj. Simic^{12a}, S. Simion¹¹⁴,

B. Simmons⁷⁶, M. Simonyan³⁵, P. Sinervo¹⁵⁷, N.B. Sinev¹¹³, V. Sipica¹⁴⁰, G. Siragusa¹⁷², A. Sircar²⁴, A.N. Sisakyan⁶⁴, S.Yu. Sivoklokov⁹⁶, J. Sjölin^{145a,145b}, T.B. Sjursen¹³, L.A. Skinnari¹⁴, H.P. Skottowe⁵⁷, K. Skovpen¹⁰⁶, P. Skubic¹¹⁰, N. Skvorodnev²², M. Slater¹⁷, T. Slavicek¹²⁶, K. Sliwa¹⁶⁰, J. Sloper²⁹, V. Smakhtin¹⁷⁰, S.Yu. Smirnov⁹⁵, L.N. Smirnova⁹⁶, O. Smirnova⁷⁸, B.C. Smith⁵⁷, D. Smith¹⁴², K.M. Smith⁵³, M. Smizanska⁷⁰, K. Smolek¹²⁶, A.A. Snesarev⁹³, S.W. Snow⁸¹, J. Snow¹¹⁰, J. Snuverink¹⁰⁴, S. Snyder²⁴, M. Soares^{123a}, R. Sobie^{168j}, J. Sodomka¹²⁶, A. Soffer¹⁵², C.A. Solans¹⁶⁶, M. Solar¹²⁶, J. Solc¹²⁶, E. Soldatov⁹⁵, U. Soldevila¹⁶⁶, E. Solfaroli Camillocci^{131a,131b}, A.A. Solodkov¹²⁷, O.V. Solovyanov¹²⁷, N. Soni², V. Sopko¹²⁶, B. Sopko¹²⁶, M. Sosebee⁷, R. Soualah^{163a,163c}, A. Soukharev¹⁰⁶, S. Spagnolo^{71a,71b}, F. Spanò⁷⁵, R. Spighi^{19a}, G. Spigo²⁹, F. Spila^{131a,131b}, R. Spiwoks²⁹, M. Spousta¹²⁵, T. Spreitzer¹⁵⁷, B. Spurlock⁷, R.D. St. Denis⁵³, T. Stahl¹⁴⁰, J. Stahlman¹¹⁹, R. Stamen^{58a}, E. Stanecka³⁸, R.W. Stanek⁵, C. Stanescu^{133a}, S. Stapnes¹¹⁶, E.A. Starchenko¹²⁷, J. Stark⁵⁵, P. Staroba¹²⁴, P. Starovoitov⁹⁰, A. Staude⁹⁷, P. Stavina^{143a}, G. Stavropoulos¹⁴, G. Steele⁵³, P. Steinbach⁴³, P. Steinberg²⁴, I. Stekl¹²⁶, B. Stelzer¹⁴¹, H.J. Stelzer⁸⁷, O. Stelzer-Chilton^{158a}, H. Stenzel⁵², S. Stern⁹⁸, K. Stevenson⁷⁴, G.A. Stewart²⁹, J.A. Stillings²⁰, M.C. Stockton⁸⁴, K. Stoerig⁴⁸, G. Stoicea^{25a}, S. Stonjek⁹⁸, P. Strachota¹²⁵, A.R. Stradling⁷, A. Straessner⁴³, J. Strandberg¹⁴⁶, S. Strandberg^{145a,145b}, A. Strandlie¹¹⁶, M. Strang¹⁰⁸, E. Strauss¹⁴², M. Strauss¹¹⁰, P. Strizenc^{143b}, R. Ströhmer¹⁷², D.M. Strom¹¹³, J.A. Strong^{75,*}, R. Stroynowski³⁹, J. Strube¹²⁸, B. Stugu¹³, I. Stumer^{24,*}, J. Stupak¹⁴⁷, P. Sturm¹⁷³, N.A. Styles⁴¹, D.A. Soh^{150,u}, D. Su¹⁴², HS. Subramania², A. Succurro¹¹, Y. Sugaya¹¹⁵, T. Sugimoto¹⁰⁰, C. Suhr¹⁰⁵, K. Suita⁶⁶, M. Suk¹²⁵, V.V. Sulin⁹³, S. Sultansoy^{3d}, T. Sumida⁶⁷, X. Sun⁵⁵, J.E. Sundermann⁴⁸, K. Suruliz¹³⁸, S. Sushkov¹¹, G. Susinno^{36a,36b}, M.R. Sutton¹⁴⁸, Y. Suzuki⁶⁵, Y. Suzuki⁶⁶, M. Svatos¹²⁴, Yu.M. Sviridov¹²⁷, S. Swedish¹⁶⁷, I. Sykora^{143a}, T. Sykora¹²⁵, B. Szeless²⁹, J. Sánchez¹⁶⁶, D. Ta¹⁰⁴, K. Tackmann⁴¹, A. Taffard¹⁶², R. Tafirout^{158a}, N. Taiblum¹⁵², Y. Takahashi¹⁰⁰, H. Takai²⁴, R. Takashima⁶⁸, H. Takeda⁶⁶, T. Takeshita¹³⁹, Y. Takubo⁶⁵, M. Talby⁸², A. Talyshev^{106,f}, M.C. Tamsett²⁴, J. Tanaka¹⁵⁴, R. Tanaka¹¹⁴, S. Tanaka¹³⁰, S. Tanaka⁶⁵, Y. Tanaka⁹⁹, A.J. Tanasijczuk¹⁴¹, K. Tani⁶⁶, N. Tannoury⁸², G.P. Tappern²⁹, S. Tapprogge⁸⁰, D. Tardif¹⁵⁷, S. Tarem¹⁵¹, F. Tarrade²⁸, G.F. Tartarelli^{88a}, P. Tas¹²⁵, M. Tasevsky¹²⁴, E. Tassi^{36a,36b}, M. Tatarkhanov¹⁴, Y. Tayalati^{134d}, C. Taylor⁷⁶, F.E. Taylor⁹¹, G.N. Taylor⁸⁵, W. Taylor^{158b}, M. Teinturier¹¹⁴, M. Teixeira Dias Castanheira⁷⁴, P. Teixeira-Dias⁷⁵, K.K. Temming⁴⁸, H. Ten Kate²⁹, P.K. Teng¹⁵⁰, S. Terada⁶⁵, K. Terashi¹⁵⁴, J. Terron⁷⁹, M. Testa⁴⁷, R.J. Teuscher^{157j}, J. Thadome¹⁷³, J. Therhaag²⁰, T. Theveneaux-Pelzer⁷⁷, M. Thioye¹⁷⁴, S. Thoma⁴⁸, J.P. Thomas¹⁷, E.N. Thompson³⁴, P.D. Thompson¹⁷, P.D. Thompson¹⁵⁷, A.S. Thompson⁵³, E. Thomson¹¹⁹, M. Thomson²⁷, R.P. Thun⁸⁶, F. Tian³⁴, M.J. Tibbetts¹⁴, T. Tic¹²⁴, V.O. Tikhomirov⁹³, Y.A. Tikhonov^{106,f}, S. Timoshenko⁹⁵, P. Tipton¹⁷⁴, F.J. Tique Aires Viegas²⁹, S. Tisserant⁸², B. Toczec³⁷, T. Todorov⁴, S. Todorova-Nova¹⁶⁰, B. Toggerson¹⁶², J. Tojo⁶⁵, S. Tokár^{143a}, K. Tokunaga⁶⁶, K. Tokushuku⁶⁶, K. Tollefson⁸⁷, M. Tomoto¹⁰⁰, L. Tompkins³⁰, K. Toms¹⁰², G. Tong^{32a}, A. Tonoyan¹³, C. Topfel¹⁶, N.D. Topilin⁶⁴, I. Torchiani²⁹, E. Torrence¹¹³, H. Torres⁷⁷, E. Torró Pastor¹⁶⁶, J. Toth^{82,aa}, F. Touchard⁸², D.R. Tovey¹³⁸, T. Trefzger¹⁷², L. Tremblet²⁹, A. Tricoli²⁹, I.M. Trigger^{158a}, S. Trincaz-Duvoid⁷⁷, T.N. Trinh⁷⁷, M.F. Tripiana⁶⁹, W. Trischuk¹⁵⁷, A. Trivedi^{24,z}, B. Trocme⁵⁵, C. Troncon^{88a}, M. Trotter-McDonald¹⁴¹, M. Trzebinski³⁸, A. Trzupek³⁸, C. Tsarouchas²⁹, J.C.-L. Tseng¹¹⁷, M. Tsiakiris¹⁰⁴, P.V. Tsiarehshka⁸⁹, D. Tsiouou^{4,ae}, G. Tsiopolitis⁹, V. Tsiskaridze⁴⁸, E.G. Tskhadadze^{51a}, I.I. Tsukerman⁹⁴, V. Tsulaia¹⁴, J.-W. Tsung²⁰, S. Tsuno⁶⁵, D. Tsybychev¹⁴⁷, A. Tua¹³⁸, A. Tudorache^{25a}, V. Tudorache^{25a}, J.M. Tuggle³⁰, M. Turala³⁸, D. Turecek¹²⁶, I. Turk Cakir^{3c}, E. Turlay¹⁰⁴, R. Turra^{88a,88b}, P.M. Tuts³⁴, A. Tykhonov⁷³, M. Tylmad^{145a,145b}, M. Tyn del¹²⁸, G. Tzanakos⁸, K. Uchida²⁰, I. Ueda¹⁵⁴, R. Ueno²⁸, M. Ugland¹³, M. Uhlenbrock²⁰, M. Uhrmacher⁵⁴, F. Ukegawa¹⁵⁹, G. Unal²⁹, D.G. Underwood⁵, A. Undrus²⁴, G. Unel¹⁶², Y. Unno⁶⁵, D. Urbaniec³⁴, G. Usai⁷, M. Uslenghi^{118a,118b}, L. Vacavant⁸², V. Vacek¹²⁶, B. Vachon⁸⁴, S. Vahsen¹⁴, J. Valenta¹²⁴, P. Valente^{131a}, S. Valentinetti^{19a,19b}, S. Valkar¹²⁵, E. Valladolid Gallego¹⁶⁶, S. Vallecorsa¹⁵¹, J.A. Valls Ferrer¹⁶⁶, H. van der Graaf¹⁰⁴, E. van der Kraaij¹⁰⁴, R. Van Der Leeuw¹⁰⁴, E. van der Poel¹⁰⁴, D. van der Ster²⁹, N. van Eldik⁸³, P. van Gemmeren⁵, Z. van Kesteren¹⁰⁴, I. van Vulpen¹⁰⁴, M. Vania dia⁹⁸, W. Vandelli²⁹, G. Vandoni²⁹, A. Vaniachine⁵, P. Vankov⁴¹, F. Vannucci⁷⁷, F. Varela Rodriguez²⁹, R. Vari^{131a}, E.W. Varnes⁶, D. Varouchas¹⁴, A. Vartapetian⁷, K.E. Varvell¹⁴⁹, V.I. Vassilakopoulos⁵⁶, F. Vazeille³³, G. Vegni^{88a,88b}, J.J. Veillet¹¹⁴, C. Vellidis⁸, F. Veloso^{123a}, R. Veness²⁹, S. Veneziano^{131a}, A. Ventura^{71a,71b}, D. Ventura¹³⁷, M. Venturi⁴⁸, N. Venturi¹⁵⁷, V. Vercesi^{118a}, M. Verducci¹³⁷, W. Verkerke¹⁰⁴, J.C. Vermeulen¹⁰⁴, A. Vest⁴³, M.C. Vetterli^{141,d}, I. Vichou¹⁶⁴, T. Vickey^{144b,af}, O.E. Vickey Boeriu^{144b}, G.H.A. Viehhauser¹¹⁷, S. Viel¹⁶⁷, M. Villa^{19a,19b}, M. Villaplana Perez¹⁶⁶, E. Vilucchi⁴⁷, M.G. Vincter²⁸, E. Vinek²⁹, V.B. Vinogradov⁶⁴, M. Virchaux^{135,*}, J. Virzi¹⁴, O. Vitells¹⁷⁰, M. Viti⁴¹, I. Vivarelli⁴⁸, F. Vives Vaque², S. Vlachos⁹, D. Vladouiu⁹⁷, M. Vlasak¹²⁶, N. Vlasov²⁰, A. Vogel²⁰, P. Vokac¹²⁶, G. Volpi⁴⁷, M. Volpi⁸⁵, G. Volpini^{88a}, H. von der Schmitt⁹⁸, J. von Loeben⁹⁸, H. von Radziewski⁴⁸, E. von Toerne²⁰, V. Vorobel¹²⁵, A.P. Vorobiev¹²⁷, V. Vorwerk¹¹, M. Vos¹⁶⁶, R. Voss²⁹, T.T. Voss¹⁷³, J.H. Vosseveld⁷², N. Vranjes^{12a}, M. Vranjes Milosavljevic¹⁰⁴, V. Vrba¹²⁴, M. Vreeswijk¹⁰⁴, T. Vu Anh⁸⁰, R. Vuillemet²⁹, I. Vukotic¹¹⁴, W. Wagner¹⁷³, P. Wagner¹¹⁹, H. Wahlen¹⁷³, J. Wakabayashi¹⁰⁰, J. Walbersloh⁴², S. Walch⁸⁶, J. Walder⁷⁰, R. Walker⁹⁷, W. Walkowiak¹⁴⁰, R. Wall¹⁷⁴, P. Waller⁷², C. Wang⁴⁴, H. Wang¹⁷¹, H. Wang^{32b,ag}, J. Wang¹⁵⁰, J. Wang⁵⁵, J.C. Wang¹³⁷, R. Wang¹⁰², S.M. Wang¹⁵⁰, A. Warburton⁸⁴, C.P. Ward²⁷, M. Warsinsky⁴⁸, P.M. Watkins¹⁷, A.T. Watson¹⁷, I.J. Watson¹⁴⁹, M.F. Watson¹⁷, G. Watts¹³⁷, S. Watts⁸¹

A.T. Waugh¹⁴⁹, B.M. Waugh⁷⁶, M. Weber¹²⁸, M.S. Weber¹⁶, P. Weber⁵⁴, A.R. Weidberg¹¹⁷, P. Weigell⁹⁸, J. Weingarten⁵⁴, C. Weiser⁴⁸, H. Wellenstein²², P.S. Wells²⁹, M. Wen⁴⁷, T. Wenaus²⁴, S. Wendler¹²², Z. Weng^{150,u}, T. Wengler²⁹, S. Wenig²⁹, N. Wermes²⁰, M. Werner⁴⁸, P. Werner²⁹, M. Werth¹⁶², M. Wessels^{58a}, C. Weydert⁵⁵, K. Whalen²⁸, S.J. Wheeler-Ellis¹⁶², S.P. Whitaker²¹, A. White⁷, M.J. White⁸⁵, S.R. Whitehead¹¹⁷, D. Whiteson¹⁶², D. Whittington⁶⁰, F. Wicek¹¹⁴, D. Wicke¹⁷³, F.J. Wickens¹²⁸, W. Wiedenmann¹⁷¹, M. Wielers¹²⁸, P. Wienemann²⁰, C. Wiglesworth⁷⁴, L.A.M. Wiik-Fuchs⁴⁸, P.A. Wijeratne⁷⁶, A. Wildauer¹⁶⁶, M.A. Wildt^{41,q}, I. Wilhelm¹²⁵, H.G. Wilkens²⁹, J.Z. Will⁹⁷, E. Williams³⁴, H.H. Williams¹¹⁹, W. Willis³⁴, S. Willocq⁸³, J.A. Wilson¹⁷, M.G. Wilson¹⁴², A. Wilson⁸⁶, I. Wingerter-Seez⁴, S. Winkelmann⁴⁸, F. Winkelmeier²⁹, M. Wittgen¹⁴², M.W. Wolter³⁸, H. Wolters^{123a,h}, W.C. Wong⁴⁰, G. Wooden⁸⁶, B.K. Wosiek³⁸, J. Wotschack²⁹, M.J. Woudstra⁸³, K.W. Wozniak³⁸, K. Wraight⁵³, C. Wright⁵³, M. Wright⁵³, B. Wrona⁷², S.L. Wu¹⁷¹, X. Wu⁴⁹, Y. Wu^{32b,ah}, E. Wulf³⁴, R. Wunstorff⁴², B.M. Wynne⁴⁵, S. Xella³⁵, M. Xiao¹³⁵, S. Xie⁴⁸, Y. Xie^{32a}, C. Xu^{32b,w}, D. Xu¹³⁸, G. Xu^{32a}, B. Yabsley¹⁴⁹, S. Yacoub^{144b}, M. Yamada⁶⁵, H. Yamaguchi¹⁵⁴, A. Yamamoto⁶⁵, K. Yamamoto⁶³, S. Yamamoto¹⁵⁴, T. Yamamura¹⁵⁴, T. Yamanaka¹⁵⁴, J. Yamaoka⁴⁴, T. Yamazaki¹⁵⁴, Y. Yamazaki⁶⁶, Z. Yan²¹, H. Yang⁸⁶, U.K. Yang⁸¹, Y. Yang⁶⁰, Y. Yang^{32a}, Z. Yang^{145a,145b}, S. Yanush⁹⁰, Y. Yao¹⁴, Y. Yasu⁶⁵, G.V. Ybeles Smit¹²⁹, J. Ye³⁹, S. Ye²⁴, M. Yilmaz^{3c}, R. Yoosofmiya¹²², K. Yorita¹⁶⁹, R. Yoshida⁵, C. Young¹⁴², S. Youssef²¹, D. Yu²⁴, J. Yu⁷, J. Yu¹¹¹, L. Yuan^{32a,ai}, A. Yurkewicz¹⁰⁵, B. Zabinski³⁸, V.G. Zaets¹²⁷, R. Zaidan⁶², A.M. Zaitsev¹²⁷, Z. Zajacova²⁹, L. Zanello^{131a,131b}, P. Zarzhitsky³⁹, A. Zaytsev¹⁰⁶, C. Zeitnitz¹⁷³, M. Zeller¹⁷⁴, M. Zeman¹²⁴, A. Zemla³⁸, C. Zender²⁰, O. Zenin¹²⁷, T. Ženiš^{143a}, Z. Zinonos^{121a,121b}, S. Zenz¹⁴, D. Zerwas¹¹⁴, G. Zevi della Porta⁵⁷, Z. Zhan^{32d}, D. Zhang^{32b,ag}, H. Zhang⁸⁷, J. Zhang⁵, X. Zhang^{32d}, Z. Zhang¹¹⁴, L. Zhao¹⁰⁷, T. Zhao¹³⁷, Z. Zhao^{32b}, A. Zhemchugov⁶⁴, S. Zheng^{32a}, J. Zhong¹¹⁷, B. Zhou⁸⁶, N. Zhou¹⁶², Y. Zhou¹⁵⁰, C.G. Zhu^{32d}, H. Zhu⁴¹, J. Zhu⁸⁶, Y. Zhu^{32b}, X. Zhuang⁹⁷, V. Zhuravlov⁹⁸, D. Zieminska⁶⁰, R. Zimmermann²⁰, S. Zimmermann²⁰, S. Zimmermann⁴⁸, M. Ziolkowski¹⁴⁰, R. Zitoun⁴, L. Živković³⁴, V.V. Zmouchko^{127,*}, G. Zobernig¹⁷¹, A. Zoccoli^{19a,19b}, Y. Zolnierowski⁴, A. Zsenei²⁹, M. zur Nedden¹⁵, V. Zutshi¹⁰⁵, L. Zwalinski²⁹

¹University at Albany, Albany NY, United States of America

²Department of Physics, University of Alberta, Edmonton AB, Canada

^{3(a)}Department of Physics, Ankara University, Ankara; ^(b)Department of Physics, Dumlupinar University, Kutahya;

^(c)Department of Physics, Gazi University, Ankara; ^(d)Division of Physics, TOBB University of Economics and Technology, Ankara; ^(e)Turkish Atomic Energy Authority, Ankara, Turkey

⁴LAPP, CNRS/IN2P3 and Université de Savoie, Annecy-le-Vieux, France

⁵High Energy Physics Division, Argonne National Laboratory, Argonne IL, United States of America

⁶Department of Physics, University of Arizona, Tucson AZ, United States of America

⁷Department of Physics, The University of Texas at Arlington, Arlington TX, United States of America

⁸Physics Department, University of Athens, Athens, Greece

⁹Physics Department, National Technical University of Athens, Zografou, Greece

¹⁰Institute of Physics, Azerbaijan Academy of Sciences, Baku, Azerbaijan

¹¹Institut de Física d'Altes Energies and Departament de Física de la Universitat Autònoma de Barcelona and ICREA, Barcelona, Spain

^{12(a)}Institute of Physics, University of Belgrade, Belgrade; ^(b)Vinca Institute of Nuclear Sciences, University of Belgrade, Belgrade, Serbia

¹³Department for Physics and Technology, University of Bergen, Bergen, Norway

¹⁴Physics Division, Lawrence Berkeley National Laboratory and University of California, Berkeley CA, United States of America

¹⁵Department of Physics, Humboldt University, Berlin, Germany

¹⁶Albert Einstein Center for Fundamental Physics and Laboratory for High Energy Physics, University of Bern, Bern, Switzerland

¹⁷School of Physics and Astronomy, University of Birmingham, Birmingham, United Kingdom

^{18(a)}Department of Physics, Bogazici University, Istanbul; ^(b)Division of Physics, Dogus University, Istanbul;

^(c)Department of Physics Engineering, Gaziantep University, Gaziantep; ^(d)Department of Physics, Istanbul Technical University, Istanbul, Turkey

^{19(a)}INFN Sezione di Bologna; ^(b)Dipartimento di Fisica, Università di Bologna, Bologna, Italy

²⁰Physikalisches Institut, University of Bonn, Bonn, Germany

²¹Department of Physics, Boston University, Boston MA, United States of America

²²Department of Physics, Brandeis University, Waltham MA, United States of America

^{23(a)}Universidade Federal do Rio De Janeiro COPPE/EE/IF, Rio de Janeiro; ^(b)Federal University of Juiz de Fora (UFJF), Juiz de Fora; ^(c)Federal University of Sao Joao del Rei (UFSJ), Sao Joao del Rei; ^(d)Instituto de Física, Universidade de Sao Paulo, Sao Paulo, Brazil

- ²⁴Physics Department, Brookhaven National Laboratory, Upton NY, United States of America
- ²⁵(a)National Institute of Physics and Nuclear Engineering, Bucharest; (b)University Politehnica Bucharest, Bucharest; (c)West University in Timisoara, Timisoara, Romania
- ²⁶Departamento de Física, Universidad de Buenos Aires, Buenos Aires, Argentina
- ²⁷Cavendish Laboratory, University of Cambridge, Cambridge, United Kingdom
- ²⁸Department of Physics, Carleton University, Ottawa ON, Canada
- ²⁹CERN, Geneva, Switzerland
- ³⁰Enrico Fermi Institute, University of Chicago, Chicago IL, United States of America
- ³¹(a)Departamento de Física, Pontificia Universidad Católica de Chile, Santiago; (b)Departamento de Física, Universidad Técnica Federico Santa María, Valparaíso, Chile
- ³²(a)Institute of High Energy Physics, Chinese Academy of Sciences, Beijing; (b)Department of Modern Physics, University of Science and Technology of China, Anhui; (c)Department of Physics, Nanjing University, Jiangsu; (d)School of Physics, Shandong University, Shandong, China
- ³³Laboratoire de Physique Corpusculaire, Clermont Université and Université Blaise Pascal and CNRS/IN2P3, Aubiere Cedex, France
- ³⁴Nevis Laboratory, Columbia University, Irvington NY, United States of America
- ³⁵Niels Bohr Institute, University of Copenhagen, Kobenhavn, Denmark
- ³⁶(a)INFN Gruppo Collegato di Cosenza; (b)Dipartimento di Fisica, Università della Calabria, Arcavata di Rende, Italy
- ³⁷AGH University of Science and Technology, Faculty of Physics and Applied Computer Science, Krakow, Poland
- ³⁸The Henryk Niewodniczanski Institute of Nuclear Physics, Polish Academy of Sciences, Krakow, Poland
- ³⁹Physics Department, Southern Methodist University, Dallas TX, United States of America
- ⁴⁰Physics Department, University of Texas at Dallas, Richardson TX, United States of America
- ⁴¹DESY, Hamburg and Zeuthen, Germany
- ⁴²Institut für Experimentelle Physik IV, Technische Universität Dortmund, Dortmund, Germany
- ⁴³Institut für Kern- und Teilchenphysik, Technical University Dresden, Dresden, Germany
- ⁴⁴Department of Physics, Duke University, Durham NC, United States of America
- ⁴⁵SUPA - School of Physics and Astronomy, University of Edinburgh, Edinburgh, United Kingdom
- ⁴⁶Fachhochschule Wiener Neustadt, Johannes Gutenbergstrasse 3, 2700 Wiener Neustadt, Austria
- ⁴⁷INFN Laboratori Nazionali di Frascati, Frascati, Italy
- ⁴⁸Fakultät für Mathematik und Physik, Albert-Ludwigs-Universität, Freiburg i.Br., Germany
- ⁴⁹Section de Physique, Université de Genève, Geneva, Switzerland
- ⁵⁰(a)INFN Sezione di Genova; (b)Dipartimento di Fisica, Università di Genova, Genova, Italy
- ⁵¹(a)E.Andronikashvili Institute of Physics, Tbilisi State University, Tbilisi; (b)High Energy Physics Institute, Tbilisi State University, Tbilisi, Georgia
- ⁵²II Physikalisches Institut, Justus-Liebig-Universität Giessen, Giessen, Germany
- ⁵³SUPA - School of Physics and Astronomy, University of Glasgow, Glasgow, United Kingdom
- ⁵⁴II Physikalisches Institut, Georg-August-Universität, Göttingen, Germany
- ⁵⁵Laboratoire de Physique Subatomique et de Cosmologie, Université Joseph Fourier and CNRS/IN2P3 and Institut National Polytechnique de Grenoble, Grenoble, France
- ⁵⁶Department of Physics, Hampton University, Hampton VA, United States of America
- ⁵⁷Laboratory for Particle Physics and Cosmology, Harvard University, Cambridge MA, United States of America
- ⁵⁸(a)Kirchhoff-Institut für Physik, Ruprecht-Karls-Universität Heidelberg, Heidelberg; (b)Physikalisches Institut, Ruprecht-Karls-Universität Heidelberg, Heidelberg; (c)ZITI Institut für technische Informatik, Ruprecht-Karls-Universität Heidelberg, Mannheim, Germany
- ⁵⁹Faculty of Applied Information Science, Hiroshima Institute of Technology, Hiroshima, Japan
- ⁶⁰Department of Physics, Indiana University, Bloomington IN, United States of America
- ⁶¹Institut für Astro- und Teilchenphysik, Leopold-Franzens-Universität, Innsbruck, Austria
- ⁶²University of Iowa, Iowa City IA, United States of America
- ⁶³Department of Physics and Astronomy, Iowa State University, Ames IA, United States of America
- ⁶⁴Joint Institute for Nuclear Research, JINR Dubna, Dubna, Russia
- ⁶⁵KEK, High Energy Accelerator Research Organization, Tsukuba, Japan
- ⁶⁶Graduate School of Science, Kobe University, Kobe, Japan
- ⁶⁷Faculty of Science, Kyoto University, Kyoto, Japan

- ⁶⁸Kyoto University of Education, Kyoto, Japan
- ⁶⁹Instituto de Física La Plata, Universidad Nacional de La Plata and CONICET, La Plata, Argentina
- ⁷⁰Physics Department, Lancaster University, Lancaster, United Kingdom
- ⁷¹(a)INFN Sezione di Lecce; (b)Dipartimento di Fisica, Università del Salento, Lecce, Italy
- ⁷²Oliver Lodge Laboratory, University of Liverpool, Liverpool, United Kingdom
- ⁷³Department of Physics, Jožef Stefan Institute and University of Ljubljana, Ljubljana, Slovenia
- ⁷⁴School of Physics and Astronomy, Queen Mary University of London, London, United Kingdom
- ⁷⁵Department of Physics, Royal Holloway University of London, Surrey, United Kingdom
- ⁷⁶Department of Physics and Astronomy, University College London, London, United Kingdom
- ⁷⁷Laboratoire de Physique Nucléaire et de Hautes Energies, UPMC and Université Paris-Diderot and CNRS/IN2P3, Paris, France
- ⁷⁸Fysiska institutionen, Lunds universitet, Lund, Sweden
- ⁷⁹Departamento de Física Teórica C-15, Universidad Autónoma de Madrid, Madrid, Spain
- ⁸⁰Institut für Physik, Universität Mainz, Mainz, Germany
- ⁸¹School of Physics and Astronomy, University of Manchester, Manchester, United Kingdom
- ⁸²CPPM, Aix-Marseille Université and CNRS/IN2P3, Marseille, France
- ⁸³Department of Physics, University of Massachusetts, Amherst MA, United States of America
- ⁸⁴Department of Physics, McGill University, Montreal QC, Canada
- ⁸⁵School of Physics, University of Melbourne, Victoria, Australia
- ⁸⁶Department of Physics, The University of Michigan, Ann Arbor MI, United States of America
- ⁸⁷Department of Physics and Astronomy, Michigan State University, East Lansing MI, United States of America
- ⁸⁸(a)INFN Sezione di Milano; (b)Dipartimento di Fisica, Università di Milano, Milano, Italy
- ⁸⁹B.I. Stepanov Institute of Physics, National Academy of Sciences of Belarus, Minsk, Republic of Belarus
- ⁹⁰National Scientific and Educational Centre for Particle and High Energy Physics, Minsk, Republic of Belarus
- ⁹¹Department of Physics, Massachusetts Institute of Technology, Cambridge MA, United States of America
- ⁹²Group of Particle Physics, University of Montreal, Montreal QC, Canada
- ⁹³P.N. Lebedev Institute of Physics, Academy of Sciences, Moscow, Russia
- ⁹⁴Institute for Theoretical and Experimental Physics (ITEP), Moscow, Russia
- ⁹⁵Moscow Engineering and Physics Institute (MEPhI), Moscow, Russia
- ⁹⁶Skobeltsyn Institute of Nuclear Physics, Lomonosov Moscow State University, Moscow, Russia
- ⁹⁷Fakultät für Physik, Ludwig-Maximilians-Universität München, München, Germany
- ⁹⁸Max-Planck-Institut für Physik (Werner-Heisenberg-Institut), München, Germany
- ⁹⁹Nagasaki Institute of Applied Science, Nagasaki, Japan
- ¹⁰⁰Graduate School of Science, Nagoya University, Nagoya, Japan
- ¹⁰¹(a)INFN Sezione di Napoli; (b)Dipartimento di Scienze Fisiche, Università di Napoli, Napoli, Italy
- ¹⁰²Department of Physics and Astronomy, University of New Mexico, Albuquerque NM, United States of America
- ¹⁰³Institute for Mathematics, Astrophysics and Particle Physics, Radboud University Nijmegen/Nikhef, Nijmegen, Netherlands
- ¹⁰⁴Nikhef National Institute for Subatomic Physics and University of Amsterdam, Amsterdam, Netherlands
- ¹⁰⁵Department of Physics, Northern Illinois University, DeKalb IL, United States of America
- ¹⁰⁶Budker Institute of Nuclear Physics, SB RAS, Novosibirsk, Russia
- ¹⁰⁷Department of Physics, New York University, New York NY, United States of America
- ¹⁰⁸Ohio State University, Columbus OH, United States of America
- ¹⁰⁹Faculty of Science, Okayama University, Okayama, Japan
- ¹¹⁰Homer L. Dodge Department of Physics and Astronomy, University of Oklahoma, Norman OK, United States of America
- ¹¹¹Department of Physics, Oklahoma State University, Stillwater OK, United States of America
- ¹¹²Palacký University, RCPTM, Olomouc, Czech Republic
- ¹¹³Center for High Energy Physics, University of Oregon, Eugene OR, United States of America
- ¹¹⁴LAL, Univ. Paris-Sud and CNRS/IN2P3, Orsay, France
- ¹¹⁵Graduate School of Science, Osaka University, Osaka, Japan
- ¹¹⁶Department of Physics, University of Oslo, Oslo, Norway
- ¹¹⁷Department of Physics, Oxford University, Oxford, United Kingdom

- ¹¹⁸(a)INFN Sezione di Pavia; (b)Dipartimento di Fisica, Università di Pavia, Pavia, Italy
- ¹¹⁹Department of Physics, University of Pennsylvania, Philadelphia PA, United States of America
- ¹²⁰Petersburg Nuclear Physics Institute, Gatchina, Russia
- ¹²¹(a)INFN Sezione di Pisa; (b)Dipartimento di Fisica E. Fermi, Università di Pisa, Pisa, Italy
- ¹²²Department of Physics and Astronomy, University of Pittsburgh, Pittsburgh PA, United States of America
- ¹²³(a)Laboratorio de Instrumentacao e Fisica Experimental de Particulas - LIP, Lisboa, Portugal; (b)Departamento de Fisica Teorica y del Cosmos and CAFPE, Universidad de Granada, Granada, Spain
- ¹²⁴Institute of Physics, Academy of Sciences of the Czech Republic, Praha, Czech Republic
- ¹²⁵Faculty of Mathematics and Physics, Charles University in Prague, Praha, Czech Republic
- ¹²⁶Czech Technical University in Prague, Praha, Czech Republic
- ¹²⁷State Research Center Institute for High Energy Physics, Protvino, Russia
- ¹²⁸Particle Physics Department, Rutherford Appleton Laboratory, Didcot, United Kingdom
- ¹²⁹Physics Department, University of Regina, Regina SK, Canada
- ¹³⁰Ritsumeikan University, Kusatsu, Shiga, Japan
- ¹³¹(a)INFN Sezione di Roma I; (b)Dipartimento di Fisica, Università La Sapienza, Roma, Italy
- ¹³²(a)INFN Sezione di Roma Tor Vergata; (b)Dipartimento di Fisica, Università di Roma Tor Vergata, Roma, Italy
- ¹³³(a)INFN Sezione di Roma Tre; (b)Dipartimento di Fisica, Università Roma Tre, Roma, Italy
- ¹³⁴(a)Faculté des Sciences Ain Chock, Réseau Universitaire de Physique des Hautes Energies - Université Hassan II, Casablanca; (b)Centre National de l'Energie des Sciences Techniques Nucleaires, Rabat; (c)Faculté des Sciences Semlalia, Université Cadi Ayyad, LPHEA-Marrakech; (d)Faculté des Sciences, Université Mohamed Premier and LTPM, Oujda; (e)Faculté des Sciences, Université Mohammed V-Agdal, Rabat, Morocco
- ¹³⁵DSM/IRFU (Institut de Recherches sur les Lois Fondamentales de l'Univers), CEA Saclay (Commissariat à l'Energie Atomique), Gif-sur-Yvette, France
- ¹³⁶Santa Cruz Institute for Particle Physics, University of California Santa Cruz, Santa Cruz CA, United States of America
- ¹³⁷Department of Physics, University of Washington, Seattle WA, United States of America
- ¹³⁸Department of Physics and Astronomy, University of Sheffield, Sheffield, United Kingdom
- ¹³⁹Department of Physics, Shinshu University, Nagano, Japan
- ¹⁴⁰Fachbereich Physik, Universität Siegen, Siegen, Germany
- ¹⁴¹Department of Physics, Simon Fraser University, Burnaby BC, Canada
- ¹⁴²SLAC National Accelerator Laboratory, Stanford CA, United States of America
- ¹⁴³(a)Faculty of Mathematics, Physics & Informatics, Comenius University, Bratislava; (b)Department of Subnuclear Physics, Institute of Experimental Physics of the Slovak Academy of Sciences, Kosice, Slovak Republic
- ¹⁴⁴(a)Department of Physics, University of Johannesburg, Johannesburg; (b)School of Physics, University of the Witwatersrand, Johannesburg, South Africa
- ¹⁴⁵(a)Department of Physics, Stockholm University; (b)The Oskar Klein Centre, Stockholm, Sweden
- ¹⁴⁶Physics Department, Royal Institute of Technology, Stockholm, Sweden
- ¹⁴⁷Departments of Physics & Astronomy and Chemistry, Stony Brook University, Stony Brook NY, United States of America
- ¹⁴⁸Department of Physics and Astronomy, University of Sussex, Brighton, United Kingdom
- ¹⁴⁹School of Physics, University of Sydney, Sydney, Australia
- ¹⁵⁰Institute of Physics, Academia Sinica, Taipei, Taiwan
- ¹⁵¹Department of Physics, Technion: Israel Inst. of Technology, Haifa, Israel
- ¹⁵²Raymond and Beverly Sackler School of Physics and Astronomy, Tel Aviv University, Tel Aviv, Israel
- ¹⁵³Department of Physics, Aristotle University of Thessaloniki, Thessaloniki, Greece
- ¹⁵⁴International Center for Elementary Particle Physics and Department of Physics, The University of Tokyo, Tokyo, Japan
- ¹⁵⁵Graduate School of Science and Technology, Tokyo Metropolitan University, Tokyo, Japan
- ¹⁵⁶Department of Physics, Tokyo Institute of Technology, Tokyo, Japan
- ¹⁵⁷Department of Physics, University of Toronto, Toronto ON, Canada
- ¹⁵⁸(a)TRIUMF, Vancouver BC; (b)Department of Physics and Astronomy, York University, Toronto ON, Canada
- ¹⁵⁹Institute of Pure and Applied Sciences, University of Tsukuba, 1-1-1 Tennodai, Tsukuba, Ibaraki 305-8571, Japan
- ¹⁶⁰Science and Technology Center, Tufts University, Medford MA, United States of America
- ¹⁶¹Centro de Investigaciones, Universidad Antonio Narino, Bogota, Colombia
- ¹⁶²Department of Physics and Astronomy, University of California Irvine, Irvine CA, United States of America

- ¹⁶³(a)INFN Gruppo Collegato di Udine, Udine; (b)ICTP, Trieste; (c)Dipartimento di Chimica, Fisica e Ambiente, Università di Udine, Udine, Italy
- ¹⁶⁴Department of Physics, University of Illinois, Urbana IL, United States of America
- ¹⁶⁵Department of Physics and Astronomy, University of Uppsala, Uppsala, Sweden
- ¹⁶⁶Instituto de Física Corpuscular (IFIC) and Departamento de Física Atómica, Molecular y Nuclear and Departamento de Ingeniería Electrónica and Instituto de Microelectrónica de Barcelona (IMB-CNM), University of Valencia and CSIC, Valencia, Spain
- ¹⁶⁷Department of Physics, University of British Columbia, Vancouver BC, Canada
- ¹⁶⁸Department of Physics and Astronomy, University of Victoria, Victoria BC, Canada
- ¹⁶⁹Waseda University, Tokyo, Japan
- ¹⁷⁰Department of Particle Physics, The Weizmann Institute of Science, Rehovot, Israel
- ¹⁷¹Department of Physics, University of Wisconsin, Madison WI, United States of America
- ¹⁷²Fakultät für Physik und Astronomie, Julius-Maximilians-Universität, Würzburg, Germany
- ¹⁷³Fachbereich C Physik, Bergische Universität Wuppertal, Wuppertal, Germany
- ¹⁷⁴Department of Physics, Yale University, New Haven CT, United States of America
- ¹⁷⁵Yerevan Physics Institute, Yerevan, Armenia
- ¹⁷⁶Domaine scientifique de la Doua, Centre de Calcul CNRS/IN2P3, Villeurbanne Cedex, France
- ¹⁷⁷Faculty of Science, Hiroshima University, Hiroshima, Japan
- ^aAlso at Laboratório de Instrumentação e Física Experimental de Partículas - LIP, Lisboa, Portugal
- ^bAlso at Faculdade de Ciências and CFNUL, Universidade de Lisboa, Lisboa, Portugal
- ^cAlso at Particle Physics Department, Rutherford Appleton Laboratory, Didcot, United Kingdom
- ^dAlso at TRIUMF, Vancouver BC, Canada
- ^eAlso at Department of Physics, California State University, Fresno CA, United States of America
- ^fAlso at Novosibirsk State University, Novosibirsk, Russia
- ^gAlso at Fermilab, Batavia IL, United States of America
- ^hAlso at Department of Physics, University of Coimbra, Coimbra, Portugal
- ⁱAlso at Università di Napoli Parthenope, Napoli, Italy
- ^jAlso at Institute of Particle Physics (IPP), Canada
- ^kAlso at Department of Physics, Middle East Technical University, Ankara, Turkey
- ^lAlso at Louisiana Tech University, Ruston LA, United States of America
- ^mAlso at Department of Physics and Astronomy, University College London, London, United Kingdom
- ⁿAlso at Group of Particle Physics, University of Montreal, Montreal QC, Canada
- ^oAlso at Department of Physics, University of Cape Town, Cape Town, South Africa
- ^pAlso at Institute of Physics, Azerbaijan Academy of Sciences, Baku, Azerbaijan
- ^qAlso at Institut für Experimentalphysik, Universität Hamburg, Hamburg, Germany
- ^rAlso at Manhattan College, New York NY, United States of America
- ^sAlso at School of Physics, Shandong University, Shandong, China
- ^tAlso at CPPM, Aix-Marseille Université and CNRS/IN2P3, Marseille, France
- ^uAlso at School of Physics and Engineering, Sun Yat-sen University, Guanzhou, China
- ^vAlso at Academia Sinica Grid Computing, Institute of Physics, Academia Sinica, Taipei, Taiwan
- ^wAlso at DSM/IRFU (Institut de Recherches sur les Lois Fondamentales de l'Univers), CEA Saclay (Commissariat à l'Energie Atomique), Gif-sur-Yvette, France
- ^xAlso at Section de Physique, Université de Genève, Geneva, Switzerland
- ^yAlso at Departamento de Física, Universidade de Minho, Braga, Portugal
- ^zAlso at Department of Physics and Astronomy, University of South Carolina, Columbia SC, United States of America
- ^{aa}Also at Institute for Particle and Nuclear Physics, Wigner Research Centre for Physics, Budapest, Hungary
- ^{ab}Also at California Institute of Technology, Pasadena CA, United States of America
- ^{ac}Also at Institute of Physics, Jagiellonian University, Krakow, Poland
- ^{ad}Also at Institute of High Energy Physics, Chinese Academy of Sciences, Beijing, China
- ^{ae}Also at Department of Physics and Astronomy, University of Sheffield, Sheffield, United Kingdom

^{af}Also at Department of Physics, Oxford University, Oxford, United Kingdom

^{ag}Also at Institute of Physics, Academia Sinica, Taipei, Taiwan

^{ah}Also at Department of Physics, The University of Michigan, Ann Arbor MI, United States of America

^{ai}Also at Laboratoire de Physique Nucléaire et de Hautes Energies, UPMC and Université Paris-Diderot and CNRS/IN2P3, Paris, France

*Deceased